

**Board B303**

Protein kinase C (PKC) can regulate  $\text{Ca}^{2+}$  sparks in vascular and airway smooth muscle cells (SMCs), but its specific molecular mechanisms remain elusive. In this study, we aimed to determine whether PKC $\epsilon$  may regulate  $\text{Ca}^{2+}$  sparks by interacting with ryanodine receptors (RyRs) and which subtype of RyRs underscores the effect of PKC $\epsilon$  in SMCs. Our data indicate that in airway SMCs, inhibition of PKC $\epsilon$  by a specific inhibitory peptide or gene deletion significantly increased the frequency of  $\text{Ca}^{2+}$  sparks, and decreased the amplitude of  $\text{Ca}^{2+}$  sparks in the presence of xestospongine-C to eliminate functional inositol 1,4,5-triphosphate receptors. PKC $\epsilon$  activation with phorbol-12-myristate-13-acetate (PMA) caused a significant decrease in  $\text{Ca}^{2+}$  spark frequency and increase in  $\text{Ca}^{2+}$  spark amplitude in the presence of xestospongine-C. The effect of PMA was completely blocked in PKC $\epsilon^{-/-}$  cells. RyR1 gene deletion abolished PKC $\epsilon$  inhibition-induced increase in  $\text{Ca}^{2+}$  spark frequency and decrease in  $\text{Ca}^{2+}$  spark amplitude. The effect of PKC $\epsilon$  activation was also prevented in RyR1 $^{-/-}$  cells. Modification of RyR2 activity by FK506-binding protein 12.6 gene deletion did not annihilate the effect of PKC $\epsilon$  inhibition and activation on either  $\text{Ca}^{2+}$  spark frequency or amplitude. PKC $\epsilon$  inhibition-elicited increase in  $\text{Ca}^{2+}$  spark frequency and decrease in  $\text{Ca}^{2+}$  spark amplitude was not eliminated in RyR3 $^{-/-}$  cells. RyR3 gene deletion did not inhibit the effect of PKC $\epsilon$  activation on  $\text{Ca}^{2+}$  sparks, either. In conclusion, PKC $\epsilon$  regulates  $\text{Ca}^{2+}$  sparks by specifically interacting with RyR1 in airway myocytes. This novel mechanism to regulate  $\text{Ca}^{2+}$  sparks may have a physiological importance in SMCs.

**Calcium Signaling Proteins****472-Pos Developing Calcium and Proteinase Sensors for Real-time Imaging**

Jenny J. Yang<sup>1</sup>, Jin Zou<sup>2</sup>, Ning Chen<sup>2</sup>, Yun Nancy Huang<sup>1</sup>, Mike Kirberger<sup>1</sup>, Shen Tang<sup>1</sup>, Yubin Zhou<sup>1</sup>, Adriana Castiblanco<sup>1</sup>, Aldberan Hofer<sup>3</sup>, April Ellis<sup>1</sup>

<sup>1</sup> Department of Chemistry, Center for Drug and Advanced Biotechnology, Georgia State University, Atlanta, GA, USA

<sup>2</sup> Department of Chemistry, Center for Drug and Advanced Biotechnology, Georgia State University, Atlanta, GA, United States, Atlanta, GA, USA

<sup>3</sup> Brigham and Women's Hospital, Harvard University, Boston, MA, USA.

**Board B304**

We demonstrate the successful design of metal-binding site in several non-metal-binding proteins with desired metal selectivity. More interestingly, these designed proteins retain their native ability to associate with natural target molecules. The solution structure reveals that designed metal binding proteins bind metal ions at the intended site with the designed arrangement, which validates our general strategy for designing de novo metal-binding proteins with multiple functionalities. The structural information also provides a close view of structural determinants that are necessary for a functional protein to accommodate the metal-binding site. Using our design approach, we have developed several fluorescent protein-based sensors with a wide range of affinities that can be applied to

monitor calcium signaling at different cellular environments and disease pathways. Different from other available sensors, our developed calcium probes have unique advantages as they do not alter the natural calcium signaling network. In addition, sensors for several different classes of proteinases, such as caspases, thrombin, trypsin, chymotrypsin, have also been developed for real-time imaging. These developed ratiometric sensors are comprised of a single fluorescent protein in contrast to other FRET based sensors which utilized paired fluorescent proteins. They are specifically ideal for monitoring cellular responses at different compartments and quantitative analysis.

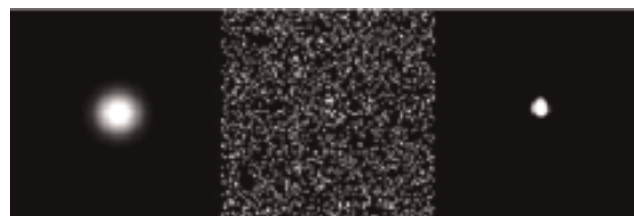
**Calcium Fluxes, Sparks and Waves****473-Pos Photo-Control of Calmodulin Binding to Target Peptide using Photochromic Compound**

Hideki Shishido, Masafumi Yamada, Kazunori Kondo, Shinsaku Maruta

SOKA univ., Tokyo, Japan.

**Board B305**

Calmodulin (CaM) is a physiologically important  $\text{Ca}^{2+}$ -binding protein that participates in numerous cellular regulatory processes. CaM has a dumbbell-like shape in which two globular domains are connected by a short  $\alpha$ -helix. Each of the globular domains has two  $\text{Ca}^{2+}$ -binding site called as EF-hand. CaM undergoes a conformational change upon binding to calcium, which enables it to bind to specific proteins for a specific response. In this study, we have demonstrated that photo-control of CaM binding to target peptide using photochromic compound N-(4-phenylazophenyl) maleimide (PAM) which undergoes *cis-trans* isomerization by ultraviolet (UV) - visible (VIS) light irradiation reversibly. PAM was incorporated into CaM mutants that have a single reactive cysteine residue. And we prepared fluorescent fusion protein M13-YFP in order to monitor interaction between CaM and M13 peptide with HPLC using size exclusion column. The binding of PAM-CaM (N60C), PAM-CaM (D64C) and PAM-CaM (M124C) to M13-YFP were apparently photo-controlled by UV-Visible light irradiation reversibly at the appropriate  $\text{Ca}^{2+}$  concentration. Interestingly, on UV light irradiation, the binding of PAM-CaM (N60C) and PAM-CaM (D64C) increased. Contrary, the binding of PAM-CaM (M124C) was decreased. And on VIS light irradiation, the binding of the PAM-CaM mutants showed opposite effect to UV light irradiation. Currently, we are trying to regulate CaM dependent enzymes using the PAM-CaM reversibly by UV-VIS light irradiation.



## 474-Pos Domain Mapping and Structural Analysis of the Cytoplasmic Tail of Polycystin-2

Edward T. Petri, Andjelka S. Celic, Barbara E. Ehrlich, Titus J. Boggon

*Yale University, New Haven, CT, USA.*

### Board B306

Inherited mutations in either *Pkd1* or *Pkd2*, the genes that encode the proteins polycystin-1 (PC1) and polycystin-2 (PC2) respectively, lead to improper function of the PC1-PC2 complex and cause polycystic kidney disease (PKD). PC1 is a receptor protein with 11 transmembrane spans and a large extracellular domain. PC2 is a 968 amino acid integral membrane protein that belongs to the transient receptor potential (TRP) channel family. PC2 functions as a  $Ca^{2+}$  permeable cation channel and is expressed in most tissues, including the kidney, heart, brain, ovaries, testis and intestine. PC2 has 6 transmembrane spans and both the C- and N-terminus are cytoplasmic. The C-terminus contains a coiled-coil domain, an EF-hand motif, four putative phosphorylation sites and an endoplasmic reticulum (ER) retention signal. PC1 and PC2 interact directly with each other and co-localize to primary cilia where they are hypothesized to be necessary for a mechanosensory response that triggers a rise in intracellular  $Ca^{2+}$ . These cytoplasmic regions are essential for function; >90% of pathogenic mutations in PC2 result in premature truncations. Using limited proteolysis we have identified two stable domains within the C-terminus of PC2. The first contains a  $Ca^{2+}$  binding domain and the second a previously unreported coiled coil domain. We have used X-ray crystallography, NMR, and Small-Angle X-ray Scattering (SAXS) to provide the first structural data for these C-terminal domains of PC2. This cytoplasmic region mediates PC2 oligomerization, the interaction of PC1 and PC2, and the interaction of PC2 with numerous downstream proteins. The structural analysis of the cytoplasmic domains of PC2 will enable a structure-guided approach to the study of PC2 mediated  $Ca^{2+}$  signaling and the molecular basis of PKD progression.

## 475-Pos Structure-Guided Functional Analysis of the Cytoplasmic Tail of Polycystin-2

Andjelka S. Celic, Edward T. Petri, Titus J. Boggon, Barbara E. Ehrlich

*Yale University, New Haven, CT, USA.*

### Board B307

Autosomal dominant polycystic kidney disease (PKD) is the most common, monogenic cause of kidney failure in humans. PKD is caused by mutations in either of two genes *Pkd1* and *Pkd2* resulting in the presence of fluid filled cysts in kidneys, liver, pancreas and intestines. The molecular mechanisms underlying PKD are unknown despite identification of the genes and mutations involved. *Pkd1* and *Pkd2* encode for the proteins, polycystin-1 (PC1) a large transmembrane protein possibly involved in cell-matrix and/or cell-

cell interactions, and polycystin-2 (PC2) a calcium ( $Ca^{2+}$ ) permeable cation channel of the transient receptor potential (TRP) family. The deletion of the carboxyl terminus of either PC1 or PC2 alters  $Ca^{2+}$  signaling. These cytoplasmic regions are essential for function; the most common pathogenic mutations are premature truncations of PC2. The addition of the extracellular agonist, vasopressin, generates  $Ca^{2+}$  transients two-fold larger in magnitude and ten times longer in duration in cells overexpressing PC2 when compared to wildtype cells, whereas deletion of the C-terminus of PC2 eliminates this effect. Using limited proteolysis and molecular modeling we have identified two stable domains within the C-terminus of PC2. The first is an EF-hand like  $Ca^{2+}$  binding domain and the second is a previously unreported coiled-coil domain. We have investigated the role of these domains in  $Ca^{2+}$  signaling *in vitro* using single channel recordings of planar lipid bilayers and *in vivo* using whole cell  $Ca^{2+}$  imaging. We hypothesize that the EF-hand domain may serve as  $Ca^{2+}$  sensor/switch, and have shown by NMR and Small-angle X-ray Scattering (SAXS) that this domain undergoes  $Ca^{2+}$  induced conformational changes and the coiled-coil domain may be responsible for PC1-PC2 and PC2-PC2 oligomerization. The correlation of structure and  $Ca^{2+}$  signaling measurements may define the role of PC2 mutations in cyst formation associated with PKD.

## 476-Pos Thermodynamic Selectivity of Calmodulin Binding to Neighboring Sites of L-type Calcium Channel Cav1.2

Turan I. Evans, Madeline A. Shea

*The University of Iowa, Iowa City, IA, USA.*

### Board B308

Cardiac L-type calcium channels (Cav1.2) play a vital role in normal heart function by regulating calcium influx. Cav1.2 is regulated by calmodulin (CaM; 148 a.a.), an essential calcium sensor, which contains two highly homologous domains; the N- (CaM1-80) and C-domain (CaM76-148). Apo (calcium-depleted) CaM is associated constitutively with Cav1.2, allowing a rapid response to increases in intracellular calcium. Upon calcium binding, CaM remains associated but undergoes conformational change and rearrangement on the channel. The cytoplasmic C-terminal tail of Cav1.2 contains 3 neighboring CaM-binding regions: a 1-8-14 motif (A), a BAA motif (C) and an IQ motif. Apo CaM is known to bind preferentially to the IQ motif. However, the nature of domain-specific interactions of CaM with these 3 regions of Cav1.2 and differences in their relative binding affinity are under debate.

We determined dissociation constants for apo and calcium-saturated CaM1-148, CaM1-80 and CaM76-148 binding to peptides representing the CaM-binding sites of Cav1.2 (A=Cav1.2p1588, C=Cav1.2p1614, and IQ=Cav1.2p1644 and Cav1.2p1650, alternate forms differing in the residues preceding IQ). The affinity of CaM1-148 for each peptide was also determined at several intermediate calcium concentrations. Cav1.2p1614, Cav1.2p1644 and Cav1.2p1650 had high affinity for CaM under high and intermediate calcium concentrations. CaM had the highest affinity for Cav1.2p1644. Consistent with the CaM-IQ interface observed crystallographically, this thermodynamic analysis showed that residues preceding the IQ-motif contributed significantly to the

energetics of recognition of Cav1.2 by CaM. The effect of each peptide on calcium-binding by CaM was determined by equilibrium calcium titration studies, and demonstrated that, unlike many IQ motifs that lower affinity, all of these peptides increased the affinity of CaM for calcium.

Supported by NIH GM57001 and F32 GM077927-01.

## 477-Pos Orai1 Subunit Stoichiometry of the Mammalian CRAC Channel Pore

Trevor J. Shuttleworth<sup>1</sup>, Olivier Mignen<sup>2</sup>, Jill L. Thompson<sup>1</sup>

<sup>1</sup> University Of Rochester Medical Center, Rochester, NY, USA

<sup>2</sup> CNRS UMR 8062, Université Paris Sud, Le Plessis-Robinson, France.

### Board B309

Recent studies have demonstrated that the protein Orai1 comprises the essential pore-forming subunit of the store-operated CRAC channels. Although evidence suggests that Orai1 can assemble as homomultimers, whether this assembly is necessary for the formation of the functional channels and, if so, the relevant stoichiometry of such multimers, is unknown. To examine this, we used an approach involving the expression of preassembled tandem Orai1 multimers comprising different numbers of subunits. Maximally-activated CRAC channel currents were recorded following transfection of these constructs in cells stably expressing STIM1. Co-expression of a dominant-negative (E106Q) Orai1 mutant allowed us to evaluate whether any recruitment of additional Orai1 units to these preassembled multimers was required for the formation of functional channels. The data obtained indicated that the trimeric construct alone cannot constitute the functional CRAC channel, whilst both the dimeric and tetrameric constructs appear capable for forming such channels. To determine which of these constitute the functional pore of the channel we replaced one of the wild-type subunits in the tetramer construct with one bearing the E106Q mutation. CRAC channel currents in cells transfected with this construct were not significantly different from those recorded in the untransfected STIM1-stable cells, demonstrating that the tetramer was not being cleaved to form dimeric channels, and that functional CRAC channels are formed specifically from a tetramer of Orai1 subunits. This was confirmed by showing that transfection of the E106Q mutant in cells stably expressing the Orai1 tetramer failed to inhibit the recorded CRAC channel currents. These data demonstrate, for the first time, that the functional CRAC channel pore is formed by a tetrameric assembly of Orai1 subunits.

## 478-Pos Oligomerization domain and stoichiometry of the CRAC channel subunit Orai

Aubin PENNA, Andriy V. YEROMIN, Olga SAFRINA, Shenyuan L. ZHANG, Michael D. CAHALAN

University of California Irvine, Irvine, CA, USA.

### Board B310

Recent RNAi screens have identified Stim (stromal interaction molecule) and Orai as critical components of the Ca<sup>2+</sup> release-

activated Ca<sup>2+</sup> (CRAC) channel in *Drosophila*. Stim functions as a sensor of luminal Ca<sup>2+</sup> content and triggers activation of CRAC channels in the surface membrane after store depletion. The CRAC channel pore domain is formed by Orai, which shares no homology with any known ion channel subunit and presents an atypical four-transmembrane domain membrane topology. It remains to be established how many Orai subunits are required to form the CRAC channel pore and where their oligomerization interface lies. In the present study, we have analyzed the quaternary structure of the Orai subunit. Co-immunoprecipitation of differently tagged Orai molecules indicated that Orai can form oligomers. Lysine- and cysteine-reactive chemical cross-linking showed that plasma membrane Orai forms multimers *in vivo* with a homodimer as a predominant form. A dimeric stoichiometry was further confirmed by a native gel system employing perfluorooctanoic acid polyacrylamide gel electrophoresis. The molecular assembly of Orai dimers was investigated by co-immunoprecipitation and chemical cross-linking of N-terminus (OraiΔNter), C-terminus (OraiΔCter) or both N- and C-termini (OraiΔNter/ΔCter) deletion mutants; these results indicated a predominant role of the transmembrane core domain in subunit assembly. Mutation of the critical E180 residue to glycine in the OraiΔNter/ΔCter core domain produced a dominant-negative inhibition of the overexpressed Stim/Orai wt-mediated CRAC current. Furthermore, using similar biochemical approaches on the expressed Orai N- and C-terminal fragments, we showed that the N-terminus of Orai represents a second, weaker interaction interface. This study suggests that the CRAC channel pore is formed by a homodimer of Orai subunits, the assembly of which is mediated mainly through the transmembrane region of each subunit and to a lesser extent by their N-terminal extremities.

## 479-Pos Stoichiometry of Stim1 and Orai1 during the assembly of CRAC channel complexes

Paul J. Hoover, Richard S. Lewis

Stanford University, Stanford, CA, USA.

### Board B311

A major fraction of Ca<sup>2+</sup> entry into non-excitable cells occurs via store-operated Ca<sup>2+</sup> channels that are activated by the depletion of Ca<sup>2+</sup> from the endoplasmic reticulum (ER). Following store depletion, the ER Ca<sup>2+</sup> sensor STIM1 and the CRAC channel subunit Orai1 reorganize from a diffuse distribution in the ER and plasma membranes into colocalized puncta separated by a cytosolic gap of only 10–25 nm (for review, see Lewis, *Nature* 446:284, 2007). The colocalization and close proximity of STIM1 and Orai1 in puncta raise the possibility that these proteins may interact with a fixed stoichiometry to evoke CRAC channel activation. To address this question, we measured the relative amounts of STIM1 and Orai1 in puncta after store depletion in HEK 293 cells. Cells were transfected with mCherry-STIM1 and eGFP-myc-Orai1, and treated with TG to deplete stores. After steady-state was reached, red and green fluorescence in each punctum was quantified by confocal imaging of the cell footprint. The red:green ratio was converted to a STIM1:Orai1 ratio by comparison with cells expressing a STIM1 variant labeled with both mCherry and eGFP. STIM1:Orai1 ratios were generally uniform across individual puncta and among all the



puncta within a cell, but varied by two-fold among cells. Formation of Orai1 puncta depends on the level of STIM1 expression, but not vice versa; thus, the observed STIM1:Orai1 ratio may be affected by the relative levels of expression of the two proteins. If this hypothesis is correct, STIM1:Orai1 ratios in cells overexpressing Orai1 relative to STIM1 will more closely represent the stoichiometry of functional STIM1-Orai1 complexes.

### **480-Pos Phosphorylation of Cardiac Calsequestrin by Protein Kinase CK2 Acts as an ER Retention Signal**

Michelle L. Milstein, Timothy P. McFarland, Saba A. Francis, Steven E. Cala

Wayne State University, Detroit, MI, USA.

#### **Board B312**

The membrane trafficking steps in heart cells that connect rough ER, junctional SR, and free SR remain unclear. In both heart and nonmuscle cells, ongoing transit of cardiac calsequestrin (cCSQ) through the secretory pathway results in its N-glycosylation on Ser-316, followed by mannose trimming in distal compartments; and phosphorylation by protein kinase CK2 on the C-terminal cluster Ser-378,382,386, which occurs co-translationally with dephosphorylation in distal compartments. In virtually all nonmuscle cells, cCSQ is found only in proximal ER cisternae. Several treatments (insertion of epitope tags, loss of luminal Ca) can cause cCSQ to escape ER retention and traffic to intermediate (ERGIC) compartments. We investigated cCSQ trafficking in several cell types using phosphorylation-site mutations: wild-type (WT) cCSQ, S(378,382,386)A (non-phosphorylated, nPP), and S(378,382,386)E (mimic (always)-phosphorylated, aPP). We combined two types of analyses, mass spectrometry to examine the pattern of CSQ molecular structures, along with fluorescence microscopy to determine subcellular localization of CSQ molecules. Mass spectrometry revealed the complete spectrum of protein structures for WT, nPP, and aPP forms of calsequestrin. Only WT CSQ showed underwent phosphorylation in intact cells. Glycosylation patterns for WT and aPP were Man<sub>9,8</sub>, indicative of early ER compartmentation. Meanwhile, the nPP mutant (Ala in place of Glu) gave a glycan pattern indicative of ERGIC trafficking, requiring its exit from proximal ER. Fluorescence microscopy data were consistent with the structural data, showing that phosphorylated CSQ (WT and aPP) was retained in ER cisternae, whereas nPP trafficked to the intermediate compartment. In conjunction with data from intact heart CSQ structure, we conclude that cCSQ is phosphorylated at the time of its biosynthesis, and this cell biological event acts to retain CSQ in the early secretory pathway. The effect of such retention in heart cells is discussed.

### **481-Pos Inhibition of Stim1 movements and activation of Orai3 by 2-aminoethyldiphenyl borate (2APB)**

Wayne I. DeHaven, Jeremy T. Smyth, Gary S. Bird, Jim W. Putney Jr.

NIEHS, RTP, NC, USA.

#### **Board B313**

Stim1 is an essential component of store-operated calcium entry (SOCE) and calcium release activated calcium currents ( $I_{crac}$ ). Stim1 functions as the calcium sensor located in the endoplasmic reticulum (ER), where dissociation of  $Ca^{2+}$  from its EF hand causes Stim1 to congregate into puncta in close proximity to the plasma membrane. 2APB is a widely used drug that biphasically activates then inhibits  $I_{crac}$ . We show here that 2APB dose dependently reverses puncta formation of EYFP-Stim1 expressed in HEK293 cells after internal calcium stores were depleted with the SERCA pump inhibitor, thapsigargin. Accordingly, 2APB also inhibited SOCE and  $I_{crac}$  in HEK-293 cells co-expressing Stim1 with the CRAC channel subunit, Orai1, and with similar potency. However, 2APB only weakly inhibited SOCE and CRAC currents in cells co-expressing Stim1 with Orai2. Further, 2APB rapidly activated calcium entry and CRAC currents in HEK-293 cells co-expressing Stim1 with Orai3. Furthermore, in cells only over-expressing Orai3, 2APB similarly activated CRAC currents and SOCE, independently of store depletion. Thus, our data suggest 2APB inhibits SOCE and  $I_{crac}$  by preventing Stim1 from forming puncta close to the plasma membrane. The activating effect of 2APB appears to be a direct action on the channels, and at least for Orai3, this occurs independently of  $Ca^{2+}$  store depletion.

### **482-Pos Mobility and Dynamics of STIM1 and Orai1 During $Ca^{2+}$ Store Depletion**

Elizabeth D. Covington, Richard S. Lewis

Stanford University, Stanford, CA, USA.

#### **Board B314**

Calcium release-activated calcium (CRAC) channels mediate calcium influx in response to depletion of calcium from the ER. Recent work has shown that upon store depletion, the ER calcium sensor STIM1 and the plasma membrane protein Orai1, a pore-forming component of the CRAC channel, translocate to sites of close apposition between the ER and plasma membranes (Luik et al., *J. Cell Biol.* 174:815, 2006). Formation of these colocalized STIM1 and Orai1 puncta leads directly to CRAC channel activation; however, little is known about the dynamic behavior of STIM1 and Orai1 puncta in the steady-state. Fluorescence recovery after photobleaching (FRAP) and photoactivation techniques were applied to fluorescently-labeled STIM1 and Orai1 expressed in HEK 293 cells to measure protein mobilities. FRAP experiments show that while GFP-STIM1 diffusion within the ER slows after store depletion by ~2-fold, GFP-Orai1 mobility is unaffected by store depletion until it forms puncta. Despite the sustained depletion of ER calcium, fluorescence within GFP-STIM1 and GFP-Orai1 puncta recovers within seconds after photobleaching, and the fluorescence of puncta labeled with a photoactivatable GFP variant bound to STIM1 or Orai1 decays after photoactivation. These results show that puncta are dynamic protein assemblies that maintain a constant size through steady-state exchange with a surrounding pool of freely diffusing protein. Mean residence times of STIM1 and Orai1 in puncta can be estimated by measuring the rate at which fluorescence

is lost from photoactivated puncta. Our results suggest the interactions of STIM1 and Orai1 within the CRAC channel activation complex are of relatively low affinity, which may limit the duration of STIM1-Orai1 interactions and hence the lifetime of the CRAC channel activated state.

### 483-Pos Contribution of Dyadic and Rogue Ryanodine Receptors to SR Ca<sup>2+</sup> Leak in Cardiac Myocytes

Aristide C. Chikando<sup>1</sup>, Eric A. Sobie<sup>2,3</sup>, W. Jon Lederer<sup>3,4</sup>, Moshin Saleet Jafri<sup>1,3</sup>

<sup>1</sup> George Mason University, Manassas, VA, USA

<sup>2</sup> Mount Sinai School of medicine, New York, NY, USA

<sup>3</sup> University of Maryland Biotechnology Institute, Baltimore, MD, USA

<sup>4</sup> University of Maryland School of Medicine, Baltimore, MD, USA.

#### Board B315

The Ca<sup>2+</sup> content of the intracellular Ca<sup>2+</sup> store in heart muscle (sarcoplasmic reticulum, SR) is dynamically controlled by a pump (the SR Ca<sup>2+</sup> ATPase, SERCA2a) and SR Ca<sup>2+</sup> release channels (ryanodine receptors, RyR2s). RyR2s are organized in large clusters (10–300 RyRs, mainly in the junctional SR, jSR) that produce Ca<sup>2+</sup> sparks and underlie the [Ca<sup>2+</sup>]<sub>i</sub> transient that regulates contraction and is isolated in single homotetrameric channels or in very small clusters (1–6 RyR2s) known as “rogue ryanodine receptors”. The totality of the Ca<sup>2+</sup> flux through RyR2s during quiescent periods constitute “SR Ca<sup>2+</sup> leak” which, when abnormal, is thought to contribute to arrhythmogenesis. To better understand the biophysical regulation of this Ca<sup>2+</sup> leak process during excitation-contraction coupling (ECC) and during diastole, in both normal and diseased settings, a mathematical model of the processes has been created (see Sobie et al. 2002). This whole cell model robustly reproduces experimentally observed graded Ca<sup>2+</sup> release and high and variable gain of ECC. The model’s simulations suggest rogue RyR2s and large clustered RyR2s have important and remarkably different kinetic features. For example, rogue RyRs contribute Ca<sup>2+</sup> efflux from the SR through brief open times (controlled by stochastic attrition) compared to dyadic large clusters (controlled by Ca<sup>2+</sup> spark kinetics). By including both rogue and large-clustered jSR RyR2s, this model presents a realistic representation of SR Ca<sup>2+</sup> flux that may provide the first molecular and cellular simulation of critical features during normal ECC and during arrhythmogenesis.

### 484-Pos H<sub>2</sub>S Regulates Intracellular Ca<sup>2+</sup> Handling via Activation of PKC in Rat Cardiomyocytes

Tingting Pan, Jinsong Bian

National University of Singapore, Singapore, Singapore.

#### Board B316

**Objective:** The present study investigated whether hydrogen sulfide (H<sub>2</sub>S) could regulate intracellular Ca<sup>2+</sup> handling in cardiomyocytes and whether Protein Kinase C (PKC) mediated this effect.

**Methods:** Freshly isolated cardiomyocytes were pretreated with NaHS (a H<sub>2</sub>S donor, 10<sup>-4</sup> M) or vehicle (control) for 30min. Dynamic changes of cytoplasmic Ca<sup>2+</sup> were visualized with a spectrofluorometric method using fura-2 ratio as an indicator. Cell fractionation and western blotting were used to assess PKC isoform translocation 20 h after NaHS treatment.

**Results:** H<sub>2</sub>S pretreatment significantly accelerated the decay of both electrically and caffeine-induced intracellular [Ca<sup>2+</sup>] transients in single cardiomyocytes and this effect was reversed by co-treatment with chelerythrine, a PKC inhibitor. This finding suggests that H<sub>2</sub>S facilitated cytoplasmic Ca<sup>2+</sup> removal in a PKC-dependant manner via both accelerating the Ca<sup>2+</sup> uptake into sarcoplasmic reticulum (SR) and enhancing Ca<sup>2+</sup> extrusion through Na<sup>+</sup>/Ca<sup>2+</sup> exchanger (NCX) on the sarcolemma membrane. The western blotting results revealed that PKCα, ε and δ abundance in membrane fraction increased two folds in H<sub>2</sub>S-pretreated cells compared with control, indicating that H<sub>2</sub>S activated these isoforms of PKC in the cardiomyocytes. Furthermore, we also observed that H<sub>2</sub>S markedly attenuated the cytoplasmic Ca<sup>2+</sup> overload during ischemia challenge due to faster clearing of Ca<sup>2+</sup> from the cytoplasm. This protective effect was abolished by inhibition of PKC.

**Conclusion:** We demonstrated for the first time that H<sub>2</sub>S ameliorates intracellular Ca<sup>2+</sup> handling via activation of PKC in cardiomyocytes. Such effect, in turn, protects the heart against ischemia injury by accelerating removal of cytoplasmic Ca<sup>2+</sup> and preventing Ca<sup>2+</sup> accumulation.

### 485-Pos Arrhythmogenic Spontaneous Ca Waves in Heart Failure Myocytes Are CaMKII-dependent

Jerry Curran<sup>1</sup>, Kathleen Hayes<sup>1</sup>, Steven Pogwizd<sup>2</sup>, Donald M. Bers<sup>3</sup>, Thomas R. Shannon<sup>1</sup>

<sup>1</sup> Rush University Medical, Chicago, IL, USA

<sup>2</sup> University of Illinois Chicago, Chicago, IL, USA

<sup>3</sup> Loyola University, Maywood, IL, USA.

#### Board B317

Increased cardiac ryanodine receptor (RyR)-dependent diastolic SR Ca leak is present in heart failure (HF) and in conditions when beta-adrenergic receptor (β-AR) tone is high. Increasing Ca leak from the SR into the cytosol could result in spontaneous Ca release (SCR) in the form of Ca waves, which activate inward Na/Ca exchanger (NCX) current causing delayed afterdepolarizations (DADs), potentially resulting in triggered arrhythmias. Here we measure SCRs in myocytes isolated from failing and control rabbit hearts. Under baseline conditions 5% of control myocytes exhibited SCR vs. 49% of cells exposed to isoproterenol (ISO, 500 nM). The ISO-induced SCR activity was reversed by CaMKII inhibitor KN-93 but not by PKA inhibitor H-89. At matching SR [Ca] ([Ca]<sub>SRT</sub>, 110 μM L<sup>-1</sup> cytosol<sup>-1</sup>) myocytes treated with ISO alone had significantly more SCRs vs. baseline (1.2±0.34 vs 0.09 ± 0.09 SCRs cell<sup>-1</sup> respectively). KN-93 reversed this increase (0.13±0.13) and H-89 did not (1.1±0.5). Of myocytes treated with forskolin 50% showed SCR activity, likely due to the observed large increase in [Ca]<sub>SRT</sub> compared to control. In HF myocytes ISO induced an enormous increase in percentage of cells showing SCRs

vs. baseline HF cells (74% vs 11%) with no significant effect on SR Ca load. This increase was prevented by KN-93 treatment (14%). At matched  $[Ca]_{SRT}$  ( $86.2 \mu M L^{-1}$  cytosol $^{-1}$ ), HF + ISO had significantly more SCRs ( $1.42 \pm 0.35 \text{ cell}^{-1}$ ) than HF untreated ( $0.23 \pm 0.13 \text{ cell}^{-1}$ ), HF + Forskolin ( $0.33 \pm 0.23 \text{ cell}^{-1}$ ) or HF+ISO+ KN93 (zero SCRs  $\text{cell}^{-1}$ ). Some myocytes stimulated by ISO showed SCRs with peak  $[Ca]_i > 90\%$  of electrically stimulated transients suggesting that spontaneous SCRs and DADs triggered action potentials. The evidence suggests increased SCR activity at high  $\beta$ -AR tone in both healthy and failing myocytes is CaMKII-dependent, implicating CaMKII in arrhythmogenesis, particularly during stress or HF.

## 486-Pos Interaction Of Calmodulin With Detergents Characterized By Fluorescence And Nmr Spectroscopy

Sankaranarayanan Srinivasan, Quinn Kleerekoper, John A. Putkey, Renhao Li

UTHSC-Houston, Houston, TX, USA.

### Board B318

Calmodulin (CaM), a ubiquitous regulatory protein in the cytoplasm, binds many transmembrane proteins to modulate their functions. The CaM-binding region in some membrane proteins is located adjacent to the transmembrane domains. Upon binding to a membrane protein, CaM may be in close contact with the cell membrane. As the first step in our study on interaction of CaM with membrane proteins, we have characterized the interaction of CaM with two commonly used detergents by fluorescence and NMR spectroscopy. Titration of both dodecyl-phosphocholine (DPC) and lysomyristoyl-phosphocholine (LMPC) to IAEDANS-labeled CaM-K75C induced an increase in IAEDANS fluorescence in the presence and absence of calcium. The apparent  $K_{dS}$  of apo-CaM and  $Ca^{2+}$ -CaM for DPC were 1–2mM, close to the critical micelle concentration (CMC) of DPC. The  $K_{dS}$  of apo-CaM and  $Ca^{2+}$ -CaM for LMPC were 1.02mM and 0.07mM, respectively. Furthermore, disappearance of most amide proton cross peaks of apo-CaM was observed when DPC was added at concentrations above its CMC, suggesting an interaction of apo-CaM with the micellar form of DPC. In contrast, significant chemical shift changes for most amide protons of  $Ca^{2+}$ -CaM could be induced by DPC at below-CMC concentrations, indicating that  $Ca^{2+}$ -CaM can bind to individual DPC molecules. The amide protons with the most chemical shift changes were mapped to both N- and C-lobes of CaM. NOESY HSQC experiments are being carried out to identify the intermolecular NOEs between CaM and detergents. Overall, these results showed that CaM interacts directly with DPC and LMPC with different characteristics. These interactions should be taken into account in studies on the interaction of CaM with membrane proteins in membrane-mimicking environments.

## 487-Pos Reduced Phospholamban Phosphorylation is Associated with Impaired Relaxation in Left Ventricular Myocytes from nNOS-Deficient Mice

Yin Hua Zhang<sup>1</sup>, Mei Hua Zhang<sup>1</sup>, Claire E. Sears<sup>1</sup>, Krzysztof Emanuel<sup>1</sup>, Charles Redwood<sup>1</sup>, Ali El-Armouche<sup>2</sup>, Evangelia G. Kranias<sup>3</sup>, Barbara Casadei<sup>1</sup>

<sup>1</sup> Department of Cardiovascular Medicine, University of Oxford, Oxford, United Kingdom

<sup>2</sup> Institute of Experimental and Clinical Pharmacology, University Hospital Eppendorf, Hamburg, Germany

<sup>3</sup> Department of Pharmacology and Cell Biophysics, University of Cincinnati College of Medicine, Cincinnati, OH, USA.

### Board B319

Stimulation of nitric oxide (NO) release from the coronary endothelium facilitates myocardial relaxation *via* a cGMP-dependent reduction in myofilament  $Ca^{2+}$  sensitivity. Recent evidence suggests that NO released by a neuronal NO synthase (nNOS) in the myocardium can also hasten left ventricular (LV) relaxation; however the mechanism underlying these findings is uncertain. Here we show that both relaxation ( $TR_{50}$ ) and the rate of  $[Ca^{2+}]_i$  transient decay ( $\tau$ ) are significantly prolonged in field-stimulated (3 Hertz) or voltage-clamped (25 ms, from -70 to +20 mV, 35°C) LV myocytes from nNOS $^{-/-}$  mice and in wild type myocytes (nNOS $^{+/+}$ ) after acute nNOS inhibition with L-VNIO (100 $\mu$ M/L). Disabling the sarcoplasmic reticulum (SR) with thapsigargin (10 $\mu$ M/L) or caffeine (10mM/L) abolished the differences in  $TR_{50}$  and  $\tau$ , suggesting that impaired SR  $Ca^{2+}$  reuptake may account for the slower relaxation in nNOS $^{-/-}$  mice. In line with these findings, disruption of nNOS (but not of endothelial NOS) decreased phospholamban phosphorylation (P-Ser<sup>16</sup> PLN), whereas nNOS inhibition had no effect on  $TR_{50}$  or  $\tau$  in PLN $^{-/-}$  myocytes. Inhibition of cGMP signaling (i.e., of soluble guanylyl cyclase, PKG) had no effect on relaxation in either group whereas PKA inhibition (PKI, 1  $\mu$ M) abolished the difference in relaxation and P-Ser<sup>16</sup> PLN by decreasing P-Ser<sup>16</sup> PLN and prolonging  $TR_{50}$  in nNOS $^{+/+}$  myocytes. Conversely, inhibition of type I or 2A protein phosphatases (inhibitor-2, 500 nM; okadaic acid, 10 nM) shortened  $TR_{50}$  and increased P-Ser<sup>16</sup> PLN in nNOS $^{-/-}$  but not in nNOS $^{+/+}$  myocytes, in agreement with data showing an increased protein phosphatase activity in nNOS $^{-/-}$  hearts.

Taken together, our findings identify a novel mechanism by which myocardial nNOS promotes LV relaxation by regulating the PKA-mediated phosphorylation of PLN and the rate of SR  $Ca^{2+}$  reuptake *via* a cGMP-independent effect on protein phosphatase activity.

## 487.01-Pos An Improved Calcium Spark Detection Algorithm

Cherrie H.T. Kong, Mark B. Cannell

University of Auckland, Auckland, New Zealand.



**Board B320**

Microscopic calcium (Ca<sup>2+</sup>) signalling events are fundamental to many cell types. In principal, a great deal of information about subcellular signal transduction can be obtained by analysing the properties of such events. However, such events (such as Ca<sup>2+</sup> sparks) are associated with low signal-to-noise ratios and are often hard to detect. Analysis of their properties is benefited by an unbiased detection system that must be sensitive and resistant to noise. To achieve this goal, we have developed an automated detector that provides a probabilistic measure of detection certainty. Sensitivity is provided by using a matched filter approach that uses a user-defined detection object. Comparing our approach to other previously published algorithms shows that the matched filter is more sensitive and more reliable.

The figure shows the detection of a synthetic Ca<sup>2+</sup> release event. The left panel shows the object to be detected, the middle panel shows the object lost in Poisson noise with a S/N of 0.5. The right panel shows the ability of the algorithm to detect the event at  $P < 0.005$ .

**487.02-Pos Quantal Dissection of Calcium Puffs**

Ian Smith<sup>1</sup>, Ian Parker<sup>2</sup>

<sup>1</sup> Univ. California, Neurobiology and Behavior, Irvine, CA, USA

<sup>2</sup> Neurobiology and Behavior, Physiology and Biophysics, Irvine, CA, USA.

**Board B321**

Calcium puffs are localized intracellular calcium transients believed to arise through the concerted openings of several clustered inositol trisphosphate receptor/channels (IP<sub>3</sub>R) to liberate calcium from ER stores. However, questions remain regarding the numbers of IP<sub>3</sub>R involved in a puff, and the mechanisms by which their activity is coordinated to initiate and terminate local calcium liberation. To address these issues, we developed imaging techniques capable of resolving calcium flux through individual IP<sub>3</sub>R during puffs in cultured SH-SY5Y neuroblastoma cells. A majority of puff sites in these cells are located adjacent to the plasma membrane, permitting use of total internal reflection microscopy to monitor near-membrane (~100 nm) calcium signals with high spatial (~300 nm) and temporal (2ms) resolution. In addition, intracellular loading with membrane-permeant EGTA-AM was used to buffer calcium, so that fluo-4 fluorescence signals more closely reflect instantaneous release flux rather than accumulation of calcium in the cytosol. Flash photolysis of membrane-permeant caged IP<sub>3</sub>-AM evoked persistent (minutes) activity at several sites per cell. Individual puff sites generally displayed a mix of 'square' quantal events that likely represent openings of single IP<sub>3</sub>R, together with larger puffs that often showed abrupt step-wise transitions on their rising and falling phases. Measurements of event and step amplitudes followed a multi-modal distribution, consistent with a quantal composition of puffs as multiples of single-IP<sub>3</sub>R calcium flux. Larger puffs had amplitudes ~8-times the quantal event indicating that they involve simultaneous openings of at least 8 IP<sub>3</sub>R. Moreover, the frequent appearance of rising and falling steps that abruptly jump several quantal levels suggests that IP<sub>3</sub>R openings and closings during puffs may not be independently stochastic, but rather that some mechanism may couple the gating of adjacent channels.

**487.03-Pos CRAC Channel-mediated Calcium Influx At The Immunological Synapse**

Maria I. Lioudyno, Debasish Sen, Aubin Penna, Shenyuan L. Zhang, Michael D. Cahalan

University of California, Irvine, Irvine, CA, USA.

**Board B322**

For efficient development of an immune response, T lymphocytes require long-lasting calcium influx through calcium release-activated calcium (CRAC) channels and the formation of a stable immunological synapse with the antigen-presenting cell. In T cells, STIM1 and Orai1 were identified as molecules essential for CRAC channel activation: Orai1 itself is a pore-subunit of the channel, whereas STIM1 serves as the ER calcium sensor which activates the CRAC channel. In human T cells and cell lines, we used live-cell imaging of GFP-tagged Orai1 and YFP-tagged STIM1, as well as confocal microscopy of immunofluorescence in fixed cells to determine the localization of STIM1 and Orai1. During basal motility, Orai1 localized to the trailing uropod within the ER and to the plasma membrane, whereas STIM1 was mostly distributed throughout the ER. Upon contact with a dendritic cell presenting superantigen, STIM1 relocated toward the edge of the T cell facing the dendritic cell, and Orai1 accumulated in the contact zone; both co-localizing in the synapse region with T cell receptor and costimulatory molecules. Furthermore, imaging of intracellular calcium in T cells, loaded with EGTA to increase buffering, revealed significantly higher calcium concentration near the interface between T cell and dendritic cell, compared to calcium concentration in the distal parts of the T cell. These data indicate that functional CRAC channels are localized to the immunological synapse. We propose that in addition to their role in global calcium signaling upon T cell activation, STIM1 and Orai1 accumulate at the immunological synapse and mediate localized calcium influx through functional CRAC channels that may play a role in immunological synapse stabilization and signal integration.

**487.04-Pos Osmotic Stress-induced Ca<sup>2+</sup> Spark Signaling Does Not Involve Changes In Cellular Redox State**

Christopher J. Ferrante, Na Li, Angela Thornton, Jianjie Ma, Noah Weisleder

UMDNJ-RWJMS, Piscataway, NJ, USA.

**Board B323**

Ca<sup>2+</sup> sparks represent elementary events of intracellular Ca<sup>2+</sup> release and can be elicited in mammalian skeletal muscle by sarcolemma permeabilization or by various stress conditions, including osmotic shock and strenuous exercise. Our laboratory has previously shown that bromoenol lactone (BEL), an iPLA2 inhibitor, could suppress the osmotic stress-induced Ca<sup>2+</sup> spark signaling in intact mammalian skeletal myofibers. Several studies have implicated the activity of iPLA2 in the production of reactive

oxygen species (ROS) in skeletal muscle. In addition, changes in redox state have been shown to modulate the activity of ryanodine receptor Ca<sup>2+</sup> release channels as well as to alter Ca<sup>2+</sup> spark activity in permeabilized mammalian skeletal myofibers. Therefore, we sought to determine the influence of cellular redox state on Ca<sup>2+</sup> spark signaling in intact mammalian skeletal myofibers. While BEL treatment reduced Ca<sup>2+</sup> spark signaling in intact flexor digitorum brevis (FDB) myofibers following either hypo- or hyper-osmotic stress, treatment with 0.1% DMSO vehicle had no effect on Ca<sup>2+</sup> spark activity. At this concentration, however, DMSO could act as a ROS scavenger and cause a reduction in cytosolic oxidant levels similar to BEL treatment. Monitoring of cellular redox state with a fluorescent ROS indicator 2',7'-dichlorodihydrofluorescein diacetate revealed no changes in cytosolic oxidant activity in FDB fibers under conditions of both hypo- and hyper-osmotic stress. In addition, persistent treatment of intact FDB myofibers with either allopurinol to inhibit xanthine oxidase, an important source of ROS, or Tiron, a ROS scavenger, had no effect on Ca<sup>2+</sup> spark signaling. These results suggest that modulation of the cytosolic redox environment does not influence the osmotic stress-induced Ca<sup>2+</sup> spark activity in mammalian skeletal muscle and that the effect of iPLA2 inhibition on Ca<sup>2+</sup> spark function does not result from changes in cellular ROS levels.

### 487.05-Pos Acute knockdown of Bin1 leads to compromised Ca spark signaling in adult skeletal muscle

Andoria Tjondrokoesoemo, Sebastian Lesniak, Christopher Ferrante, Jaekyun Ko, Noah Weisleder, Jianjie Ma

*Robert Wood Johnson Medical School, Piscataway, NJ, USA.*

#### Board B324

We previously showed that mice null for MG29 display reduced Ca spark frequency in skeletal muscle following osmotic stress stimulation, a phenotype similar to that observed in aged wild type muscle (*J. Cell Biol.* **174**:639, 2006). This finding, coupled with decreased expression of MG29 in aged skeletal muscle, suggests that reduced MG29 expression could be one factor that contributes to altered intracellular Ca signaling in aging skeletal muscle. Here we show that Bin1 is an interacting partner for MG29. Previous studies have shown that both MG29 and Bin1 are involved in maintenance of transverse-tubule (TT) membrane structures in skeletal muscle, however the functional impact of Bin1 on Ca signaling in skeletal muscle has not been studied, largely due to the fact that genetic ablation of Bin1 leads to neonatal lethality in mice. We used electroporation to introduce shRNA against Bin1 (shRNA-Bin1) into the flexor digitorum brevis (FDB) muscle of viable mice, to produce acute knockdown of Bin1 in adult skeletal muscle. Using DiOC5 fluorescent dye that labels TT membranes in FDB fibers, we found that integrity of the TT membrane structure was maintained in muscle fibers transfected with shRNA-Bin1 compared with those transfected with the control shRNA. Fibers transfected with shRNA-Bin1 lacked hypo-osmotic stress induced Ca spark responses, in contrast to the robust Ca spark activity observed in FDB muscle fiber

transfected with the control shRNA. Moreover, reduced Ca spark frequency upon hyper-osmotic treatment was observed. Our findings suggest that Bin1 may directly influence the intracellular Ca release machinery in skeletal muscle. We are currently investigating the role of Bin1-MG29 interaction in mediating the changes in triad-junction ultrastructure and/or direct effects on Ca spark signaling machinery in muscle physiology and aging.

### 487.06-Pos Functional And Structural Consequences Of Transiently Increasing Calsequestrin Concentration By ~700% In Mouse Skeletal Muscle

Leandro Royer<sup>1</sup>, Sandrine Pouvreau<sup>1</sup>, Ying Wang<sup>2</sup>, Gerhard Meissner<sup>2</sup>, Jingsong Zhou<sup>1</sup>, Pompeo Volpe<sup>3</sup>, Alessandra Nori<sup>3</sup>, Robert Fitts<sup>4</sup>, James W. Bain<sup>5</sup>, Danny A. Riley<sup>5</sup>, Eduardo Rios<sup>1</sup>

<sup>1</sup> Rush University, Chicago, IL, USA

<sup>2</sup> University of North Carolina, Chapel Hill, NC, USA

<sup>3</sup> Universita degli Studi di Padova, Padova, Italy

<sup>4</sup> Marquette University, Milwaukee, WI, USA

<sup>5</sup> Medical College of Wisconsin, Milwaukee, WI, USA.

#### Board B325

Calsequestrin, predominantly as isoform 1, is the most abundant Ca-binding protein of the sarcoplasmic reticulum of skeletal muscle, where it is believed to constitute the main store of functionally releasable Ca. It is also thought to dynamically modulate RyR channel gating, in a [Ca<sup>2+</sup>]<sub>SR</sub>-dependent manner. Using a technique of DiFranco et al. (2006) we transiently modified the content of CSQ1 in the SR of fast twitch muscle of living adult mice. A plasmid that also coded for EGFP caused the content to increase by 700%, as determined by Western blots of fluorescent cells. Fusions of CSQ1 and CFP or YFP had a similar cellular distribution as that of fluorescently tagged anti-CSQ1 antibodies in control muscles, namely double strands of protein flanking Z disks around myofibrils. When both fusions were transfected simultaneously, they had identical distribution and exhibited FRET, indicating polymerization. Electron microscopy revealed numerous large membrane sacs filled with dense clumped material, presumably CSQ1, in the Golgi region and deeper in the fiber, where they formed triad junctions. Ca transients and release flux were studied under voltage clamp. There was no correlation between total releasable Ca and over-expression density (as measured by marker fluorescence). No difference in the kinetics of Ca release was found between expressing and non-expressing cells. Releasable Ca estimated by challenges with chloro-m-cresol was increased by 28% (±9%) in 22 CSQ1-over-expressing intact cells loaded with indo-5F. These effects will be compared with those of silencing the CSQ1 gene, resulting in a greater than 20-fold reduction of its expression (Royer et al. this meeting). In conclusion, massive transient increases of CSQ1 result in a minimal addition to the functionally releasable Ca pool.

Supported by NIAMS/NIH.



## 487.07-Pos Comparison Of Voltage-dependent And Voltage-independent $\text{Ca}^{2+}$ Sparks In Frog Skeletal Muscle Fibers

Henrietta Cserne Szappanos<sup>1</sup>, Yingfan Zhang<sup>2</sup>, Shawn P. Mullen<sup>2</sup>, Michael G. Klein<sup>2</sup>, Martin F. Schneider<sup>2</sup>

<sup>1</sup> University of Debrecen, Debrecen, Hungary

<sup>2</sup> University of Maryland Baltimore, Baltimore, MD, USA.

### Board B326

In frog skeletal muscle,  $\text{Ca}^{2+}$  sparks occur both as voltage-dependent and voltage-independent (ligand-activated) release events. We compared the properties of voltage-dependent  $\text{Ca}^{2+}$  sparks during depolarization with voltage-independent sparks. Voltage-dependent sparks were evoked by long duration (1750 ms) small depolarizations (e.g., from  $-90$  to  $-60$  mV) of voltage clamped cut frog fibers or by 5–10 min exposure of intact frog fibers to elevated  $\text{K}^+$  solution for high time resolution recording. The properties of voltage-independent spontaneous sparks and voltage-dependent sparks from the same fiber were compared in either cut or intact fibers. In fully polarized cut fibers,  $\text{Ca}^{2+}$  spark frequency showed an exponential increase of e-fold for every 3.6 mV of applied depolarization. During depolarization, the resting calcium level did not change and the spark amplitude remained unchanged in both cut and intact fibers, but the temporal half duration and the spatial half width increased (from 6.11 to 6.48 vs 6.07 to 7.68 ms and from 1.15 to 1.3 vs. 1.1 to 1.61  $\mu\text{m}$  respectively, for cut fibers vs. intact fibers). Based on the increase of the spatial half width, the area of the sparks became larger. The difference in half width between voltage-dependent and -independent  $\text{Ca}^{2+}$  sparks might indicate that more RyRs may be involved in voltage-dependent sparks, possibly explained by junctional RyRs coupled to DHPRs not being involved in the generation of voltage-independent sparks, whereas at least one coupled RyR must be involved in each voltage-dependent spark. The 2 dimensional spatial distribution of both voltage-dependent and -independent  $\text{Ca}^{2+}$  sparks is currently under investigation using high speed xy imaging.

## 487.08-Pos TIRF Imaging Of $\text{Ca}^{2+}$ -Induced $\text{Ca}^{2+}$ Release In Smooth Muscle Cells

Hisao Yamamura

Nagoya City University, Nagoya, Japan.

### Board B327

In smooth muscles, cytosolic  $\text{Ca}^{2+}$  ( $[\text{Ca}^{2+}]_i$ ) dynamics during an action potential are triggered by  $\text{Ca}^{2+}$  influx through voltage-dependent  $\text{Ca}^{2+}$  channel (VDCC) in plasma membrane. The physiological significance of  $\text{Ca}^{2+}$  amplification by subsequent  $\text{Ca}^{2+}$  release through ryanodine receptor (RyR) from sarcoplasmic reticulum (SR) is still a matter of topics in smooth muscles. In the present

study, depolarization-evoked local  $\text{Ca}^{2+}$  transients ( $\text{Ca}^{2+}$  hot spots) via  $\text{Ca}^{2+}$ -induced  $\text{Ca}^{2+}$  release (CICR) through RyR on subplasmalemmal SR in smooth muscle cells of murine urinary bladder were imaged using a total internal reflection fluorescence (TIRF) microscope. Upon depolarization from a holding potential of  $-60$  to  $0$  mV for 50 ms under whole-cell voltage-clamp, the rapid elevation of  $[\text{Ca}^{2+}]_i$  (as fluo-4 signals) occurred in a limited TIRF zone less than 200 nm from the chamber bottom, and the rate of  $[\text{Ca}^{2+}]_i$  change reached the peak within 16 ms. The depolarization-evoked  $[\text{Ca}^{2+}]_i$  increase in TIRF zone was abolished by the pretreatment with  $100 \mu\text{M Cd}^{2+}$  or  $10 \mu\text{M}$  ryanodine. The depolarization-induced outward currents, which were simultaneously recorded with  $\text{Ca}^{2+}$  images, were mainly due to the activation of large-conductance  $\text{Ca}^{2+}$ -activated  $\text{K}^+$  (BK) channels, and were also reduced by these blockers. When myocytes were stained with DM-BODIPY (-)-dihydropyridine ( $0.1 \mu\text{M}$ ) or specific  $\alpha 1\text{C}$  antibody (1:100), the fluorescent signals of individual channel unit or their clusters were not uniformly distributed in the TIRF images and the sum of fluorescent areas occupied approximately 1 % of the plasma membrane in the image. These TIRF analyses are useful to visualize and quantify the CICR due to unit  $\text{Ca}^{2+}$  influx and elucidate its physiological significance in excitation-contraction (EC) coupling in smooth muscles.

(Supported by Grant-in-Aids from the Ministry of Education, Culture, Sports, Science and Technology and the Japan Society for the Promotion of Sciences)

## 487.09-Pos Interstitial Cells from Cerebral Arteries Belong to Smooth Muscle Cell Phenotype

Maksym I. Harhun, Holger Laux, Sally A. Prestwich, Dmitri V. Gordienko, Thomas B. Bolton

St. George's, University of London, London, United Kingdom.

### Board B328

It is now established that non-contractile cells with thin processes, also called vascular interstitial cells (ICs), are constitutively present in the media of blood vessel walls. The aim of this study was to determine the cell phenotype to which arterial ICs belong using immunocytochemical, and real-time and reverse transcription PCR (RT-PCR). Using RT-PCR we compared gene expression profiles of single ICs and smooth muscle cells (SMCs) freshly dispersed from rat middle cerebral artery. Both ICs and SMCs expressed the SMC marker, smooth muscle myosin heavy chain (SM-MHC), but did not express fibroblast, pericyte, neuronal, mast cell, endothelial or stem cell markers. Vascular ICs also did not express c-kit, which is the marker for Interstitial Cells of Cajal in the gastrointestinal tract. Immunocytochemical staining of isolated ICs and SMCs showed that both types of cell expressed the contractile proteins  $\alpha$ -SM actin and SM-MHC. However, the expression of calponin, which is another protein participating in contraction of SMC, was almost undetectable in ICs. Since RT-PCR showed the presence of all three protein transcripts in both cell types, single IC and SMC cDNA was pre-amplified and subsequently used in real-time PCR. This showed

4 times higher gene expression of calponin in SMCs comparing to ICs, which may explain ICs inability to contract.

Immunocytochemical studies also showed that both cell types have similar expression of structural proteins such as  $\beta$ -actin, vinculin and  $\alpha$ -actinin. However the expression of desmin, which is unique to muscle and endothelial cells, was significantly higher in ICs than in SMCs. The results obtained suggest that ICs originate from the same precursor as SMCs, but later develop a non-contractile cell phenotype with processes.

Supported by Wellcome Trust (042293, 074724, 075112); M.I.H. is British Heart Foundation IBSR Fellow (FS/06/077)

### 487.10-Pos Up-on-its-side Orientation of Adult Ventricular Myocytes for the Confocal Structure/Function Analysis of the T-tubular System And $\text{Ca}^{2+}$ Dynamics

Norbert Klauke, Nial MacQuaide, Jonathan M Cooper, Godfrey L Smith

*Uni Glasgow, Glasgow, United Kingdom.*

#### Board B329

The x-y resolution of the confocal microscope is higher than the z resolution. Biophysical investigations of the functional adult ventricular myocyte would benefit from the ability to place the brick-shaped cell on its side to exploit the better xy resolution for longitudinal sections across the narrower cell width. Here we describe a high aspect ratio microfluidic channel with matching dimensions of the cardiomyocyte width where the channel walls prevent the cell from settling flat on the coverslip. The open channels were fabricated on microscope coverslips with integrated platinum microelectrodes for the electrical stimulation to evoke action potentials and concomitant  $\text{Ca}^{2+}$  transients. Cells were continually superfused with saline solution passed through the length of the channel. 3D-reconstructions of the dye-loaded t-tubular system (SNARF-1) of a cell-on-its-side were compared with 3D-reconstructions from flat cells. The confocal z-scans of side-oriented cells show a regular array of radial tubules entering from both sides with matching registration but not making contact with each other in the same plane of focus.  $\text{Ca}^{2+}$  release events, e.g. sparks, transients and waves were recorded in side-oriented cells with 2-P excitation of Fluo-3 and Fluo-5N. The spatial and temporal profiles of these events were compared with those from flat-oriented cells. The results were fed into a computational model of the  $\text{Ca}^{2+}$  wave to predict the minimum number of sparks needed for the initiation of a  $\text{Ca}^{2+}$  wave.

### 487.11-Pos Quantification Of SR Depletion During Spontaneous $\text{Ca}^{2+}$ Waves In Ventricular Cardiomyocytes

Niall Macquaide, Godfrey L. Smith

*University of Glasgow, Glasgow, United Kingdom.*

#### Board B330

During  $\text{Ca}^{2+}$  overload, cardiomyocytes exhibit spontaneous waves of  $\text{Ca}^{2+}$  release from the SR. Previous work suggests that  $\text{Ca}^{2+}$  waves do not empty the SR completely, estimates of depletion range from 45–80% of the SR  $\text{Ca}^{2+}$ . The degree of SR depletion during a  $\text{Ca}^{2+}$  wave was examined in this study. Isolated rabbit ventricular myocytes were incubated with Fluo5N AM. These were subsequently permeabilised using  $\beta$ -escin and studied using fluorescence confocal microscopy. The cardiomyocytes were perfused using a mock intracellular solution containing ~600nM free  $\text{Ca}^{2+}$  (50 $\mu\text{M}$  EGTA), this caused regular  $\text{Ca}^{2+}$  waves (0.8-1Hz). These signals were compared with the complete SR depletion on caffeine (10mM) application. In line-scan mode, spontaneous  $\text{Ca}^{2+}$  waves were evident as transient decreases of fluorescence. The amplitude of the transient decrease in fluorescence during a wave was  $21\pm 3\%$  of the response seen in caffeine. Quantification of the local SR  $\text{Ca}^{2+}$  depletion during the wave was assessed using the following set of corrections:

- (i) offsetting for wave velocity
- (ii) converting fluorescence to free SR [ $\text{Ca}^{2+}$ ]
- (iii) conversion to total SR [ $\text{Ca}^{2+}$ ].

These calculations suggest that the mean local SR depletion during  $\text{Ca}^{2+}$  waves was  $92\pm 5\%$  of that during caffeine (n=10). This indicates that the majority of SR  $\text{Ca}^{2+}$  is released locally during a  $\text{Ca}^{2+}$  wave. Similar values were obtained using signals from a cytoplasmic indicator (Fluo5F). Reduction of RyR sensitivity using tetracaine (50 $\mu\text{M}$ ) increased SR content and  $\text{Ca}^{2+}$  wave amplitude, but the relative depletion of the SR similarly complete. A computational model was created using these SR characteristics. This model was able to reproduce the burst phenomenon observed on transiently increasing RyR sensitivity that previously had been attributed to partial SR depletion.

### 487.12-Pos K201 Inhibits Diastolic $\text{Ca}^{2+}$ Release And Contractions In Isolated Rat Cardiomyocytes Without Increasing Subsequent Transient Amplitude

Elsbeth B.A. Elliott<sup>1</sup>, Toshiya Matsuda<sup>2</sup>, Noboru Kaneko<sup>2</sup>, Christopher M. Loughrey<sup>1</sup>, Godfrey L. Smith<sup>1</sup>

<sup>1</sup> *University of Glasgow, Glasgow, United Kingdom*

<sup>2</sup> *Dokkyo University School of Medicine, Tochigi, Japan.*

#### Board B331

Previous work has shown that the drug K201 (Aetas Pharma, Japan) may have an anti-arrhythmic action through its effect on the ryanodine receptor (RyR2). The current study examined the effect of 1 $\mu\text{M}$  K201 on diastolic  $\text{Ca}^{2+}$  release events (DREs) and diastolic contractile events (DCEs) in isolated rat cardiomyocytes under  $\text{Ca}^{2+}$  overload conditions. Cells loaded with Fura-4 AM were field stimulated at 2.5Hz (37°C) on the stage of an inverted microscope. Simultaneous measurements of intracellular  $\text{Ca}^{2+}$  (expressed in terms of fluorescence ratio) using epifluorescence and fractional cell shortening (L/L<sub>0</sub>; IonOptix) were made.  $\text{Ca}^{2+}$  overload (4.75mM  $\text{Ca}^{2+}$  and 150nM isoproterenol) resulted in the appearance of DREs

and DCEs between stimuli. Following 3–4min K201 application, a significant reduction in mean  $\text{Ca}^{2+}$  transient amplitude was observed ( $0.47 \pm 0.05$  vs.  $0.37 \pm 0.05$ ; 340/380nm;  $p < 0.05$ ;  $n = 8$ ). Mean stimulated fractional shortening amplitude was also significantly reduced by K201 ( $0.119 \pm 0.014$  vs.  $0.097 \pm 0.014$ ;  $L/L_o$ ;  $p < 0.05$ ;  $n = 8$ ). Importantly, K201 produced a significant inhibition of the amplitudes of diastolic  $\text{Ca}^{2+}$  release ( $0.18 \pm 0.03$  vs.  $0.05 \pm 0.02$ ; 340/380nm;  $p < 0.05$ ;  $n = 8$ ) and diastolic fractional shortening ( $0.049 \pm 0.007$  vs.  $0.009 \pm 0.004$ ;  $L/L_o$ ;  $p < 0.01$ ;  $n = 8$ ). In a subset of cells ( $n = 4$ ), DREs were completely abolished by K201. The relationship between the amplitude of preceding DRE and amplitude of stimulated  $\text{Ca}^{2+}$  transient in  $\text{Ca}^{2+}$  overload was examined. Linear extrapolation of this relationship predicted that inhibition of DREs would cause a  $32 \pm 12\%$  increase in transient amplitude. However, inhibition of DREs with K201 was associated with a reduction in amplitude of  $15 \pm 8\%$  ( $p < 0.01$ ). These data suggest that the effects of K201 on intracellular  $\text{Ca}^{2+}$  signals cannot be explained only in terms of inhibition of diastolic  $\text{Ca}^{2+}$  release.

### 487.13-Pos Sparking up Spiral Calcium Waves in a Single Heart Cell

Aihui Tang<sup>1</sup>, Yong-Qiang Bai<sup>2</sup>, Xing Zhu<sup>2</sup>, Shi-Qiang Wang<sup>1</sup>

<sup>1</sup> College of Life Sciences, Peking University, Beijing, China

<sup>2</sup> School of Physics, Peking University, Beijing, China.

#### Board B332

Spiral waves are ubiquitously found in physical, chemical and biological systems. Spiral waves in heart tissues are implicated in the genesis of ventricular fibrillation, a severe arrhythmia causing unpredictable sudden death. Studies using biological and chemical systems have led to a detailed understanding of spiral wave dynamics, but much less are known about the natural origin of spiral waves. Part of the limitation is the lack of a suitable experimental model to identify the very early microscopic events leading to spiral waves. Utilizing the state-of-the-art live-cell imaging technology, we can now visualize micron-scale spiral waves of intracellular  $\text{Ca}^{2+}$  together with the elementary  $\text{Ca}^{2+}$  release events,  $\text{Ca}^{2+}$  sparks, in a single cardiac cell. We found that  $\text{Ca}^{2+}$  sparks are not only the fundamental building blocks of  $\text{Ca}^{2+}$  waves, but also internal triggers of  $\text{Ca}^{2+}$  spirals. While solitary  $\text{Ca}^{2+}$  sparks interact with wave fronts in a stochastic manner, a portion of them have a chance to initiate spiral waves. Phase mapping analysis showed that a spiral-generating spark comes with a pair of topological defects, known as phase singularities, which are required as engines of spiral waves. Notably, phase singularity pairs could only be generated when the  $\text{Ca}^{2+}$  spark hits an existing wave at a specific range of phase, dubbed “singularity zone”. When the singularity zone is expanded by factors promoting  $\text{Ca}^{2+}$  sparks, e.g., over-dosage of catecholamine under  $\text{Ca}^{2+}$  overloaded conditions, the enhanced genesis of phase singularities brings on numerous regional spirals, putting intracellular  $\text{Ca}^{2+}$  into chaotic activities. These results demonstrate experimentally for the first time that internal stochasticity may provide triggers for the re-entrant dynamics in a discrete system, and reveal that a new level of hierarchical complexity may underlie the genesis of cardiac arrhythmia.

### 487.14-Pos A Role of Type 1 Inositol 1,4,5-Trisphosphate Receptors in Activating Peri-nuclear $\text{Ca}^{2+}$ Sparks in HL-1 Atrial Myocytes

Joon-Chul Kim<sup>1</sup>, Sunwoo Lee<sup>1</sup>, Yuhua Li<sup>1</sup>, Min-Jeong Son<sup>1</sup>, Do Han Kim<sup>2</sup>, Joung Real Ahn<sup>3</sup>, Sun-Hee Woo<sup>1</sup>

<sup>1</sup> Chungnam National University, Daejeon, Republic of Korea

<sup>2</sup> GIST, Gwangju, Republic of Korea

<sup>3</sup> Sungkyunkwan University, Suwon, Republic of Korea.

#### Board B333

HL-1 cells are adult mouse atrial myocytes that continuously divide and spontaneously beat. We examined the spatio-temporal characteristics of focal  $\text{Ca}^{2+}$  releases in HL-1 cells and a possible role of inositol 1,4,5-trisphosphate receptors ( $\text{IP}_3\text{R}$ ) in the regulation of the focal releases using confocal microscopy. Immunocytochemistry revealed punctate even distributions of type 2 ryanodine receptors throughout the cytoplasm in these myocytes. Spontaneous focal  $\text{Ca}^{2+}$  releases, which were sensitive to caffeine and ryanodine, were observed at the non-junctional (central), junctional (peripheral) and peri-nuclear sites. The frequency (events/ $[10^3 \mu\text{m}^2\text{s}]$ ) of the  $\text{Ca}^{2+}$  sparks was  $\sim 0.3$  in the center,  $\sim 2.5$  in the periphery and  $\sim 9$  at the peri-nucleus with 2-D imaging at 2.38 Hz. The peripheral sparks were brighter and wider than the central and peri-nuclear sparks. Central sparks lasted shorter than others, and peri-nuclear sparks developed much more slowly compared to central or peripheral sparks. Some of the peripheral and peri-nuclear  $\text{Ca}^{2+}$  sparks were repetitively activated from the same spots. The occurrences of peri-nuclear  $\text{Ca}^{2+}$  sparks were dramatically reduced in type 1  $\text{IP}_3\text{R}$  knock-down cells but not in type 2  $\text{IP}_3\text{R}$  knock-down cells. The central and peripheral spark occurrences were not affected by type 1 or type 2  $\text{IP}_3\text{R}$  knock-down. These results indicate that HL-1 cells possess three kinds of functional  $\text{Ca}^{2+}$  release sites with distinct subcellular localizations and spatio-temporal properties, and suggest a role of type 1  $\text{IP}_3\text{R}$  in the activation of peri-nuclear  $\text{Ca}^{2+}$  release sites.

### 487.15-Pos Fluo-3 In The Mitochondrial Intermembrane Space

Valeriy Lukyanenko<sup>1</sup>, Tatiana Rostovtseva<sup>2</sup>, W. Jonathan Lederer<sup>1</sup>

<sup>1</sup> UMBI, Baltimore, MD, USA

<sup>2</sup> Laboratory of Physical and Structural Biology, NICHD, National Institutes of Health, Bethesda, MD, USA.

#### Board B334

Mitochondrial  $\text{Ca}^{2+}$  cycling could be involved in the regulation of sarcoplasmic reticulum (SR)  $\text{Ca}^{2+}$  cycling in cardiomyocytes, given its proximity to the SR and known  $\text{Ca}^{2+}$  dependent function and potential  $\text{Ca}^{2+}$  storage capacity. Recently we showed that fluo-3 pentapotassium salt (fluo-3<sup>5-</sup>) enters the mitochondrial intermembrane space (MIMS) and fluoresces more brightly there than in the surrounding solution. This observation may prove useful in dynamic studies of mitochondria diameter (i.e. mitochondrial swelling) and MIMS and SR  $\text{Ca}^{2+}$  cycling. Here we examined why fluo-3<sup>5-</sup> is so



fluorescent in the MIMS using both confocal and planar lipid bilayer experiments.

Experiments were carried out using isolated rat cardiac mitochondria to study characteristics of fluo-3 and voltage dependent anion channel (VDAC) reconstituted into planar lipid membranes to study permeability of VDAC for fluo-3. We show that there can be a  $[Ca^{2+}]$ -dependent increase in the fluorescence of fluo-3<sup>5-</sup> in the MIMS. This MIMS signal from fluo-3 and one from the extra-mitochondrial solution for fluo-3 have the same  $K_d$  for the  $Ca^{2+}$ . Additionally, we show that VDAC is permeable to fluo-3<sup>5-</sup>, a finding supported by the effect that known VDAC inhibitors, DIDS and König's polyanion, prevent MIMS loading by fluo-3<sup>5-</sup>. In contrast, the putative VDAC blockers Ru360 or La<sup>3+</sup> did not prevent the filling of the MIMS with fluo-3<sup>5-</sup>. That the increased fluorescence from fluo-3 in MIMS may be due to MIMS environmental factors is suggested by experiments with  $Ca^{2+}$ -independent fluorochromes (calcein and sulforhodamine B).

We conclude that fluo-3<sup>5-</sup> may be used as a probe for cardiac VDAC in its original membrane environment and under quasi-physiological conditions. Our working hypothesis is that the enhanced fluo-3<sup>5-</sup> fluorescence in the MIMS arises from a higher apparent concentration of fluo-3<sup>5-</sup> in MIMS.

## 488-Pos Propagation of $Ca^{2+}$ Waves in Ventricular Myocytes: SR Versus Cytosolic Activation Of RyR2 Channels

Hena R. Ramay<sup>1</sup>, Mohsin S. Jafri<sup>2</sup>, W J. Lederer<sup>3</sup>, Eric A. Sobie<sup>1</sup>

<sup>1</sup> Mount Sinai School of Medicine, New York, NY, USA

<sup>2</sup> George Mason University, Fairfax, VA, USA

<sup>3</sup> University of Maryland Biotechnology Institute, Baltimore, MD, USA.

### Board B335

Under pathological conditions such as  $Ca^{2+}$  overload spontaneous calcium ( $Ca^{2+}$ ) sparks in ventricular myocytes can give rise to regenerative  $Ca^{2+}$  waves whereby sparks trigger additional sparks from neighboring clusters of sarcoplasmic reticulum (SR)  $Ca^{2+}$  release channels (ryanodine receptors; RyR2s). Controversy exists, however, regarding the relative roles played by 1) cytosolic diffusion of  $Ca^{2+}$  and activation of neighboring RyR2 clusters through  $Ca^{2+}$ -induced  $Ca^{2+}$  release versus 2) cluster-to-cluster diffusion of  $Ca^{2+}$  within the SR network sensitizing RyRs at sites that have not yet been activated (un-activated sites). We explored these possibilities through simulations with a computer model.

Using a spatial computational model of multiple  $Ca^{2+}$  release sites, we simulated  $Ca^{2+}$  movements during waves by opening RyR2 clusters for fixed durations at specified times.  $Ca^{2+}$  dynamics in the cytosol and SR are governed by diffusion, buffers, release through RyR2s and uptake by SERCA (SR  $Ca^{2+}$ -ATPase) pumps. Parameters that we modulated included  $Ca^{2+}$  diffusion coefficients in the cytosol ( $D_{Ca,cyto}$ ) and SR ( $D_{Ca,SR}$ ), SERCA pump distribution, and partial block of SERCA.

Our preliminary results (with  $D_{Ca,cyto} = 250 \mu m^2/s$ ) suggest that if SR diffusion is fast ( $D_{Ca,SR} = 300 \mu m^2/s$ ) a decrease in  $[Ca^{2+}]_{SR}$  at un-activated RyR2 clusters is observed due to  $Ca^{2+}$  diffusion towards depleted SR regions (i.e. activated sites). SR  $[Ca^{2+}]$  at un-activated RyR2 clusters will increase if  $D_{Ca,SR}$  is small ( $12 \mu m^2/s$ ) largely due to SERCA pump uptake near un-activated RyR2

clusters rather than  $Ca^{2+}$  diffusion within the SR. These results suggest that SR-dependent RyR2 sensitization at un-activated sites could influence  $Ca^{2+}$  wave propagation but its contribution depends on  $Ca^{2+}$  diffusion within the SR and the spatial distribution of SERCA pumps.

## 489-Pos How Does the Diastolic Calcium Sparks Frequency Depend on the Sarcoplasmic Reticulum Calcium Content in Mouse Cardiac Cells?

Julio Altamirano, W. Jonathan Lederer

Med. Biotech. Ctr., Univ. Maryland Biotech. Inst., Baltimore, MD, USA.

### Board B336

Upon electrical stimulation of cardiac myocytes, a small sarcolemmal  $Ca^{2+}$  influx locally controls larger  $Ca^{2+}$  release events ( $Ca^{2+}$  sparks) from the sarcoplasmic reticulum (SR), due to the activation of clusters of  $Ca^{2+}$ -release channels (RyR2). However, even in quiescent cells spontaneous  $Ca^{2+}$  sparks occur, albeit at a low frequency, contributing to "SR  $Ca^{2+}$  leak" ( $SR_{Leak}$ ). Such  $Ca^{2+}$  sparks depend on the SR  $Ca^{2+}$  content ( $[Ca^{2+}]_{SR}$ ), and an apparently steep non linear relation between the  $Ca^{2+}$  sparks frequency (CaSpF) and  $[Ca^{2+}]_{SR}$  has been suggested. However, the simultaneous measurements of  $[Ca^{2+}]_{SR}$  and  $Ca^{2+}$  sparks have not been performed, especially during dynamic regulation of  $[Ca^{2+}]_{SR}$ . Furthermore, it has been suggested that excessive PKA-dependent phosphorylation (PKA-P) of RyR2 during heart failure (HF) enhances the RyR2  $P_{open}$ , thereby increasing  $SR_{Leak}$ , which might help to explain the lower  $[Ca^{2+}]_{SR}$ . However, cellular studies, at steady state  $[Ca^{2+}]_{SR}$ , showed that enhanced PKA-P did not increase CaSpF. To directly measure the  $[Ca^{2+}]_{SR}$ , a low affinity  $Ca^{2+}$  indicator (Mag-Fluo-4) was loaded into the SR of intact phospholamban knock out (PLB-KO) mouse myocytes. Rhod-2 was used to simultaneously monitor  $Ca^{2+}$  sparks in saponin-permeabilized cells. The relationship between  $[Ca^{2+}]_{SR}$  and CaSpF was measured as  $[Ca^{2+}]_{SR}$  increased following caffeine application. This relationship was found to be steeply non linear. Application of cAMP slightly decreased steady state CaSpF without significantly changing  $[Ca^{2+}]_{SR}$ . Additionally, cAMP did not change the rate of  $Ca^{2+}$  sparks restoration following caffeine application and did not greatly affect the relation CaSpF vs.  $[Ca^{2+}]_{SR}$ . We conclude that while the  $Ca^{2+}$  spark-dependent  $SR_{Leak}$  is significantly dependent on  $[Ca^{2+}]_{SR}$ , it is not increased by RyR2 PKA-P.

## 490-Pos Energetic State Is A Strong Regulator Of The SR Leak In Cardiac Muscle: Different Efficiencies Of Different Energy Sources

Malle Kuum<sup>1,2</sup>, Allen Kaasik<sup>2</sup>, Frederic Joubert<sup>1</sup>, Renée Ventura-Clapier<sup>1</sup>, Vladimir Veksler<sup>1</sup>

<sup>1</sup> Univ. Paris-Sud, INSERM U-769, Châtenay-Malabry, France

<sup>2</sup> Univ. of Tartu, Tartu, Estonia.

**Board B337**

Increased diastolic SR  $\text{Ca}^{2+}$  leak at high intracellular/extracellular calcium ratios could depress contractility in heart failure. Since the failing myocardium has impaired energetics, we investigated in permeabilized preparations how SR  $\text{Ca}^{2+}$  leak depends on different energetic conditions: exogenous ATP (3.16 mM), ATP+12 mM phosphocreatine, ATP+mitochondrial substrates (mitochondrial activation), or with all of these together (optimal energetic conditions). SR was  $\text{Ca}^{2+}$ -loaded for 5 min at pCa 6.5 under optimal energetic conditions, then leakage was assessed under different energetic conditions in  $\text{Ca}^{2+}$ -free solution. In rat cardiomyocytes loaded with the fluorescent marker mag-fluo-4, the decline in SR  $[\text{Ca}^{2+}]$  was more than two times faster in the presence of exogenous ATP only than under optimal energetic conditions. In mouse ventricular fibers, caffeine-induced tension transients under optimal energetic conditions were used to estimate SR  $\text{Ca}^{2+}$  content. Taking SR  $\text{Ca}^{2+}$  content after 5 min incubation without  $\text{Ca}^{2+}$  under optimal energetic conditions as 100%, we found that in the presence of exogenous ATP only, the SR  $\text{Ca}^{2+}$  content declined to  $27 \pm 5\%$ . Activation of endogenous creatine kinase (CK) by phosphocreatine significantly increased SR  $\text{Ca}^{2+}$  content after the leak period to  $52 \pm 5\%$  ( $p < 0.001$ ). Mitochondrial activation was even more effective in preventing  $\text{Ca}^{2+}$  leak, such that SR  $\text{Ca}^{2+}$  content rose to  $88 \pm 8\%$  ( $p < 0.01$  vs CK system). The significant leak with only exogenous ATP was not inhibited by the ryanodine receptor blockers tetracaine or ruthenium red. However, the SERCA inhibitors cyclopiazonic acid and TBQ significantly decreased  $\text{Ca}^{2+}$  leak. In conclusion, the data obtained suggest that at low extracellular  $[\text{Ca}^{2+}]$

1. the main leak pathway is an energy-sensitive backward  $\text{Ca}^{2+}$  pump, and
2. direct mitochondrial-SERCA ATP channelling is more effective in leak prevention than local ATP generation by bound CK.

### **491-Pos Altered Redox-Modulation of Ryanodine Receptors Associated with Ca-transient Alternans in a Canine Model of Sudden Cardiac Death**

Andriy Belevych, Dmitry Terentyev, Zuzana Kubalova, Serge Viatchenko-Karpinski, Arun Sridhar, Carlos del Rio, Yoshinori Nishijima, Cynthia A. Carnes A. Carnes, George E. Billman, Sandor Gyorke

*The Ohio State University, Columbus, OH, USA.*

**Board B338**

Ventricular arrhythmias remain a major cause of death following myocardial infarction (MI). Although alterations in intracellular Ca cycling are recognized as an important contributor to the pathogenesis of ventricular arrhythmias, the specific cellular and molecular mechanisms of these alterations remain to be defined. We investigated the potential role and underlying causes of changes in intracellular Ca handling in arrhythmia using a post-MI canine model of ischemia-induced ventricular fibrillation (VF). Intracellular Ca cycling was monitored in the cytosolic ( $[\text{Ca}]_c$ ) and SR compartments ( $[\text{Ca}]_{\text{SR}}$ ) in isolated intact and permeabilized ven-

tricular myocytes using confocal microscopy and patch-clamp techniques. Myocytes isolated from the VF group exhibited a significantly higher frequency of spontaneous Ca waves and Ca sparks than control cells. These changes in spontaneous Ca release signals were associated with a significant reduction in  $[\text{Ca}]_{\text{SR}}$  indicative of elevated SR Ca leakage due to increased functional activity of RyR channels. When rhythmically paced, myocytes from both VF and control groups displayed beat-to-beat alternations in the amplitude of  $[\text{Ca}]_c$  transients (Ca alternans) and action potential duration.  $[\text{Ca}]_{\text{SR}}$  always oscillated in phase with the alternans of Ca transient amplitude. In VF myocytes the frequency-dependence of Ca alternans was significantly shifted to lower frequencies and alternans at a given frequency occurred at lower  $[\text{Ca}]_{\text{SR}}$  with respect to control cells from non-infarcted hearts. The parameters of cytosolic and luminal Ca signals in VF myocytes were almost completely normalized by the reducing agents dithiothreitol (1 mM) and mercaptopropionylglycine (1 mM). These results suggest that increased functional activity of RyRs caused by redox modifications promotes generation of Ca and action potential alternans, thereby providing an arrhythmogenic substrate in post-infarction hearts.

### **492-Pos Purinergic Signaling Governs Intracellular Ca Oscillations and Contractility in Early Cardiogenesis**

Serge Viatchenko-Karpinski, Sandor Gyorke

*Ohio State University Medical Center, Columbus, OH, USA.*

**Board B339**

Spontaneous oscillations in intracellular  $[\text{Ca}]$  ( $[\text{Ca}]_i$ ) and contractile state are intrinsic features of cardiac myocytes beginning from very early stages of development. To determine the underlying molecular and subcellular mechanisms of intracellular Ca oscillations in early cardiogenesis, we performed confocal fluorescence measurements of intracellular Ca dynamics in embryonic stem (ES, murine D3 cell line) cells derived from multicellular aggregates (embryoid bodies, EB). Undifferentiated ES cells and contracting early cardiomyocytes (ECMs) exhibited spontaneous Ca oscillations. The characteristics of these signals were not influenced neither by high extracellular potassium (50mM  $\text{K}^+$ ) nor by Ca channel and sodium-calcium exchange blockers SV-6 (10 $\mu\text{M}$ ) or  $\text{Ni}^+$  (1mM), thus, revealing their intracellular origin. Application of ATP (100 $\mu\text{M}$ ) elevated baseline  $[\text{Ca}]_i$  and increased both the frequency and magnitude of Ca oscillations in undifferentiated ES cells and contracting ECMs. The spontaneous Ca oscillations and ATP-induced Ca responses in both cell types were prevented by the P2 purino-receptor (R) antagonist suramin (100 $\mu\text{M}$ ). Application of the selective type P2XR agonist 8-Br-ATP (300 $\mu\text{M}$ ) resulted in an elevation of baseline  $[\text{Ca}]_i$  in both ES cells and ECMs without causing/affecting Ca oscillations. At the same time, activation of the P2YR by the specific agonist uridine 5'-diphosphate (UDP, 1mM) increased the frequency and amplitude of Ca oscillations without altering baseline  $[\text{Ca}]_i$ . Qualitatively similar effects on  $[\text{Ca}]_i$  were obtained on stimulation of the IP3R stores by endothelin-1 (100 $\mu\text{M}$ ). Application of the RyR activator, caffeine (10mM), induced a brief and small elevation in  $[\text{Ca}]_i$  in all ECMs but not ES cells without affecting any parameters of the spontaneous Ca

oscillations in either cell type. Taken together, these results suggest that intracellular calcium oscillations and contractility in early cardiogenesis are mediated by type P2YR functionally linked to intracellular IP<sub>3</sub>R Ca stores.

### **493-Pos Expression, Subcellular Localization and Functional Characteristics of Inositol 1,4,5-Trisphosphate Receptor Subtypes in HL-1 Atrial Myocytes**

Joon-Chul Kim, Sunwoo Lee, Min-Jeong Son, Yuhua Li, Sun-Hee Woo

*College of Pharmacy, Chungnam National University, Daejeon, Republic of Korea.*

#### **Board B340**

We examined the functional expression of inositol 1,4,5-trisphosphate receptor (IP<sub>3</sub>R) in HL-1 adult atrial cell line. RT-PCR and western blot analyses revealed expression of type 1 IP<sub>3</sub>R (IP<sub>3</sub>R1) and type 2 IP<sub>3</sub>R (IP<sub>3</sub>R2) in HL-1 cells, which was similar to the expressions of these subtypes in intact atrial cells but contrasted with the presence of IP<sub>3</sub>R2 in ventricular cells. Expression level of the IP<sub>3</sub>R1 was 2.5-fold higher in HL-1 cells compared to intact atrial cells, while that of IP<sub>3</sub>R2 was similar in HL-1 and intact atrial cells. Immunostaining of the IP<sub>3</sub>R subtypes displayed peri-nuclear localization of IP<sub>3</sub>R1 and even distribution of punctate IP<sub>3</sub>R2 at the cytoplasm. Exposures of saponin-permeabilized HL-1 cells to IP<sub>3</sub> (20 μM) elicited transient Ca<sup>2+</sup> increases at the cytoplasm and at the nucleus. The IP<sub>3</sub>-induced nuclear Ca<sup>2+</sup> rises had larger latencies and amplitudes compared to the cytoplasmic Ca<sup>2+</sup> increases. When Ca<sup>2+</sup> increased to a level relatively higher than the resting level during the exposure to IP<sub>3</sub> (20 μM), oscillatory Ca<sup>2+</sup> waves were observed at the cytoplasm in a subset of cells tested. We also observed IP<sub>3</sub>-induced focal release events at the cytoplasm in the presence of high concentrations of ryanodine. The IP<sub>3</sub>-induced Ca<sup>2+</sup> releases were inhibited by pre-exposures to the blockers of IP<sub>3</sub>R, heparin or 2-APB. These results provide an evidence for molecular and functional expressions of IP<sub>3</sub>R1 and IP<sub>3</sub>R2 in HL-1 cells, and suggest that the slow delayed nuclear Ca<sup>2+</sup> rise and cytoplasmic oscillatory Ca<sup>2+</sup> release may be mediated by IP<sub>3</sub>R1 and IP<sub>3</sub>R2, respectively. Distinct physiological roles of IP<sub>3</sub>R subtypes in HL-1 cells and their functional similarities to those of intact atrial pacemaker cells need further investigations.

### **494-Pos A Moment Closure Approach to Modeling Local Control of Calcium-Induced Calcium Release in Cardiac Myocytes**

Marco Huertas<sup>1</sup>, George S. B. Williams<sup>1</sup>, Eric A. Sobie<sup>2</sup>, Saleet Jafri<sup>3</sup>, Gregory D. Smith<sup>1</sup>

<sup>1</sup> *Department of Applied Science, College of William and Mary, Williamsburg, VA, USA*

<sup>2</sup> *Department of Pharmacology and Systems Therapeutics, Mount Sinai School of Medicine, New York, NY, USA*

<sup>3</sup> *Department of Bioinformatics and Computational Biology, George Mason University, Manassas, VA, USA.*

#### **Board B341**

In prior work we introduced a probability density approach to modeling local control of Ca-induced Ca release in cardiac myocytes [Williams et al. *Biophys. J.* 92(7):2311–28, 2007] where coupled advection-reaction equations described the time-dependent probability density of subsarcolemmal subspace and junctional sarcoplasmic reticulum [Ca] conditioned on Ca release unit (CaRU) state. When coupled to ODEs for the bulk myoplasmic and network SR [Ca], a realistic but minimal model of cardiac excitation-contraction coupling is produced that avoids the computationally demanding task of resolving spatial aspects of global Ca signaling, while accurately representing heterogeneous local Ca signals in a population of diadic subspaces and junctional sarcoplasmic reticulum depletion domains. Here we introduce a computationally efficient method for approximately simulating such whole cell models that begins with a derivation of a system of ODEs describing the time-evolution of the first and second moments of the probability density functions for local [Ca] jointly distributed with CaRU state. This open system of ODEs is then closed by assuming an algebraic relationship that expresses the third moment in terms of the first and second moments. In simulated voltage-clamp protocols using four-state CaRUs that respond to the dynamics of junctional SR depletion, this “moment closure approach” to modeling local control of excitation-contraction coupling produces high-gain Ca release that is graded with changes in membrane potential, a phenomenon not exhibited by so-called “common pool” models. Benchmark simulations indicate that the moment closure approach is 9700 times more computationally efficient than corresponding Monte Carlo simulations and leads to nearly identical results.

### **495-Pos Spatial Properties Of Ca Sparks And Ca Transients In Atrial And Ventricular Myocytes Recorded With High-Speed 2-Dimensional Confocal Microscopy**

Vyacheslav M. Shkryl, Lothar A. Blatter

*Loyola University Chicago, Maywood, IL, USA.*

#### **Board B342**

In cat atrial and ventricular myocytes Ca sparks and Ca transients were recorded with high-speed, 2-dimensional confocal microscopy (>1000 frames/s; Zeiss LSM 5 LIVE). Ca sparks had variable spatial properties depending on subcellular location. In atrial myocytes sparks recorded from the central regions (corresponding to Ca release from non-junctional SR) were on average spatially symmetrical with full-width at half-maximum amplitude in longitudinal direction (FWHM<sub>long</sub>) of 2.8±0.1 μm (n=30 sparks) and 2.7±0.1 μm in transverse direction (FWHM<sub>trans</sub>). The symmetry ratio (FWHM<sub>long</sub>/FWHM<sub>trans</sub>) was 1.06±0.03. Ca sparks originating from junctional SR in subsarcolemmal regions were anisotropic



with a  $\text{FWHM}_{\text{long}}/\text{FWHM}_{\text{trans}}$  ratio of  $1.71 \pm 0.05$  which was mainly due to reduced spatial spread in the transverse direction ( $\text{FWHM}_{\text{long}} = 2.5 \pm 0.1 \mu\text{m}$ ;  $\text{FWHM}_{\text{trans}} = 1.5 \pm 0.1 \mu\text{m}$ ;  $n=30$ ). After cell membrane permeabilization with saponin the  $\text{FWHM}_{\text{long}}/\text{FWHM}_{\text{trans}}$  ratio of peripheral atrial sparks decreased to  $1.45 \pm 0.1$ , consistent with the structural disruption of the arrangement of sarcolemma, SR membrane and ryanodine receptor Ca release channels in the diadic cleft of the peripheral couplings of the junctional SR. The symmetry of spatial spread of central sparks was not affected by permeabilization. In ventricular myocytes peripheral and central sparks had a  $\text{FWHM} = 2.9 \pm 0.1 \mu\text{m}$  in both dimension and a  $\text{FWHM}_{\text{long}}/\text{FWHM}_{\text{trans}}$  ratio of  $1.01 \pm 0.03$ . Ca transients in response to electrical field stimulation caused an initial release of Ca from peripheral junctional SR release sites in form of discrete Ca sparks that showed the same anisotropy as peripheral spontaneous Ca sparks. Within  $<10$  ms discrete peripheral sparks fused into a peripheral ring of elevated  $[\text{Ca}]_i$  that subsequently propagated in a wave-like fashion towards the center of the cell. In ventricular myocytes discrete Ca sparks with no preferential sub-cellular location preceded the electrically evoked whole-cell Ca transient.

### 496-Pos The Role Of Mitochondria In Generation Of Spontaneous $\text{Ca}^{2+}$ Waves In Cat Atrial Myocytes

Aleksey V. Zima, Lothar A. Blatter

*Loyola University Chicago, Maywood, IL, USA.*

#### Board B344

We studied the relationship between energetic state of mitochondria and spontaneous  $\text{Ca}^{2+}$  waves in cat atrial myocytes during sarcoplasmic reticulum (SR)  $\text{Ca}^{2+}$  overload. Depolarization of the mitochondrial membrane with FCCP led to an initial, nearly complete inhibition of  $\text{Ca}^{2+}$  wave frequency, followed by a recovery that remained below control level (55%). The initial phase associated with an increase in SR  $\text{Ca}^{2+}$  load whereas the recovery was paralleled by a decrease of load. In the presence of the  $\text{F}_1\text{F}_0$ -ATPase blocker oligomycin, FCCP had only a stimulatory effect on  $\text{Ca}^{2+}$  waves, with a frequency increase of  $\sim 200\%$ . Oligomycin, however, did not abolish the depolarizing effect of FCCP on mitochondrial membrane potential. The augmentation of  $\text{Ca}^{2+}$  wave frequency was dependent on external  $\text{Ca}^{2+}$ , but not L-type  $\text{Ca}^{2+}$  channel activity. FCCP caused an initial increase in intracellular  $\text{Mg}^{2+}$  concentration ( $[\text{Mg}^{2+}]_i$ ) followed by a decline to a stable plateau above control level. Oligomycin abolished the initial FCCP-induced rise in  $[\text{Mg}^{2+}]_i$  suggesting that this effect was mediated in part by ATP hydrolysis due to  $\text{F}_1\text{F}_0$ -ATPase acting in reverse mode. Inhibition of glycolysis abolished the recovery of  $[\text{Mg}^{2+}]_i$  and caused an irreversible contracture. Collapse of the mitochondrial membrane potential with FCCP also led to cytosolic acidification and accumulation of intracellular  $\text{Na}^+$  ( $[\text{Na}^+]_i$ ). Inhibition of sarcolemmal  $\text{Na}^+$ - $\text{H}^+$  exchange with cariporide ( $5 \mu\text{M}$ ) partially prevented the increase of  $\text{Ca}^{2+}$  wave frequency produced by FCCP and oligomycin. These results suggest that mitochondrial depolarization affects spontaneous  $\text{Ca}^{2+}$  waves via several mechanisms: ATP hydrolysis and accumulation of free  $[\text{Mg}^{2+}]$  inhibit ryanodine receptor-mediated SR  $\text{Ca}^{2+}$  release; this effect is partially counteracted by glycolytic

ATP production. Subsequent accumulation of  $[\text{Na}^+]_i$  reduces  $\text{Ca}^{2+}$  extrusion via  $\text{Na}^+$ - $\text{Ca}^{2+}$  exchange, leading to cytosolic  $\text{Ca}^{2+}$  overload and an increase in the propensity of  $\text{Ca}^{2+}$  waves.

### 497-Pos Spark and non-Spark mediated SR Calcium Leak in Rabbit Ventricular Myocytes

Aleksey V. Zima, Eckard Picht, Donald M. Bers, Lothar A. Blatter

*Loyola University Chicago, Maywood, IL, USA.*

#### Board B345

Quantification of calcium sparks is used to determine ryanodine receptor (RyR)-mediated diastolic sarcoplasmic reticulum (SR) Ca leak. We tested the hypothesis that non-spark mediated SR Ca release also contributes to diastolic Ca leak. We simultaneously measured intra-SR free Ca ( $[\text{Ca}]_{\text{SR}}$ ) with Fluo-5N and cytosolic Ca sparks with Rhod-2 in permeabilized rabbit ventricular myocytes. SR Ca leak ( $d[\text{Ca}]_{\text{SR-total}}/dt$ ) was measured after complete SERCA inhibition by thapsigargin. Spark frequency, amplitude and width were steeply  $[\text{Ca}]_{\text{SR}}$ -dependent. Initially upon SERCA blockade,  $[\text{Ca}]_{\text{SR}}$ , leak and Ca spark frequency declined in concert. When  $[\text{Ca}]_{\text{SR}}$  declined to  $\sim 40\%$  of control, spark activity ceased, but SR Ca leak continued unabated (and declined along with  $[\text{Ca}]_{\text{SR}}$ ). The  $[\text{Ca}]_{\text{SR}}$  threshold for spark cessation was similar to minimal local  $[\text{Ca}]_{\text{SR}}$  depletions during individual sparks. Thus Ca sparks may stop at the same  $[\text{Ca}]_{\text{SR}}$  where release normally terminates. To test if this spark-independent leak still occurred through RyRs, we completely inhibited RyRs with tetracaine, Mg or ruthenium red. RyR inhibition in the absence of thapsigargin increased SR Ca load to  $264 \pm 10\%$ , confirming that RyRs provide an important leak pathway. During SERCA inhibition, RyR blockers inhibited Ca sparks, but did not abolish SR Ca leak, suggesting the existence of RyR-independent leak.  $\text{IP}_3$ -receptors were not responsible for the RyR-independent leak pathway as neither  $\text{IP}_3$  nor the  $\text{IP}_3$ -receptor antagonist heparin significantly altered SR Ca leak in the presence of RyR inhibition. These results indicate that RyRs are the main, but not the sole contributor to SR Ca leak. RyR-mediated leak occurs in part as Ca sparks, but there is clearly RyR-mediated leak that is not observable as Ca sparks. Additionally, there may be quantitatively important SR Ca leak that is RyR- and  $\text{IP}_3$ -independent, but the molecular pathway remains to be determined.

### 498-Pos Developmental Alterations in SR Structure and Function in Ventricular Myocytes

Andrew P. Ziman, Julio Altamirano, W J. Lederer

*University of Maryland Biotechnology Institute, Baltimore, MD, USA.*

#### Board B346

Excitation-contraction coupling (ECC) links electrical to mechanical activity in heart.  $\text{Ca}^{2+}$  influx through voltage-gated  $\text{Ca}^{2+}$

channels (dihydropyridine receptor, DHPR) in the sarcolemma (SL) activate clusters of SR Ca<sup>2+</sup> release channels (ryanodine receptors, RyR2) in the sarcoplasmic reticulum (SR) to trigger Ca<sup>2+</sup> release. In adult ventricular myocytes the elementary unit of SR Ca<sup>2+</sup> release during ECC is the Ca<sup>2+</sup> spark, however Ca<sup>2+</sup> sparks also occur at a very low rate due to RyR2 openings at diastolic cytosolic [Ca<sup>2+</sup>]<sub>i</sub>. Clusters of DHPRs and RyR2s are found plentifully in and adjacent to the transverse tubules. ECC structures change during development and these alterations lead to parallel changes in function. We have examined these developmental changes in rat ventricular myocytes from early postnatal development (postnatal day 10) to adult maturity (at least 6 weeks). We have used a combination of confocal Ca<sup>2+</sup> imaging (using fluo-4) and immunofluorescence to investigate how changes in ECC-related proteins affect Ca<sup>2+</sup> signaling. The junctional SR and network SR were imaged in living cells using the low affinity Ca<sup>2+</sup> indicator mag-fluo-4. The RyR2s are the core element of a macromolecular complex (MMC) that regulates SR Ca<sup>2+</sup> release, and therefore we have examined critical proteins of this MMC, including SR luminal protein calsequestrin as well as RyR2 itself. We find that during postnatal development of the SR, Ca<sup>2+</sup> handling changes to meet the needs of the maturing myocyte. These new insights into ECC development broaden our understanding of Ca<sup>2+</sup> signaling dysfunction in adult ventricular myocytes that undergo de-differentiation.

### 499-Pos Initiation of Ca<sup>2+</sup> Release Events by Local Increases in Intraluminal Sarcoplasmic Reticulum [Ca<sup>2+</sup>]<sub>i</sub> in Murine Ventricular Myocytes

Brian M. Hagen, Jiahong Ni, Joseph P.Y. Kao, W. Jonathan Lederer

*University of Maryland Biotechnology Institute, Baltimore, MD, USA.*

#### Board B347

The sarcoplasmic reticulum (SR) in cardiac myocytes is a Ca<sup>2+</sup> cycling organelle comprised of interconnected tubules, and is the major source of the Ca<sup>2+</sup> released during contraction and the sink into which Ca<sup>2+</sup> is pumped during relaxation. The elementary event of SR Ca<sup>2+</sup> release is the Ca<sup>2+</sup> spark which occurs when a cluster of ryanodine receptors (RyR2, SR Ca<sup>2+</sup> release channels) in the SR are activated. While the Ca<sup>2+</sup> spark is normally thought to be triggered by local [Ca<sup>2+</sup>]<sub>i</sub> increase in the subspace between the SR and the sarcolemmal (SL) membranes by an influx of Ca<sup>2+</sup> through at least one L-type Ca<sup>2+</sup> channel, other possibilities have been suggested. To examine how Ca<sup>2+</sup> sparks may be activated, we examine Ca<sup>2+</sup> spark triggering using a newly created caged Ca<sup>2+</sup> (PGTA) and local (subcellular) UV illumination. PGTA can be introduced specifically into the SR of cardiac ventricular myocytes or into the cytosol. Using graded release of Ca<sup>2+</sup> in these two distinct compartments with photolysis, we were able to identify under what conditions Ca<sup>2+</sup> sparks could be initiated. While under normal conditions Ca<sup>2+</sup> sparks do not trigger other Ca<sup>2+</sup> sparks from neighboring clusters of RyR2, in diverse diseases they do and may produce propagating waves of elevated Ca<sup>2+</sup>. The new technology that has enabled us to investigate Ca<sup>2+</sup> spark initiation has also enabled us to examine how

Ca<sup>2+</sup> sparks initiate Ca<sup>2+</sup> waves within ventricular myocytes. This characterization of Ca<sup>2+</sup> sparks and Ca<sup>2+</sup> waves lays the foundation for a broader understanding of normal and abnormal Ca<sup>2+</sup> signaling within the heart. Among the important new findings of this work is the clear ability of a step increase in SR [Ca<sup>2+</sup>]<sub>i</sub> to instantly activate Ca<sup>2+</sup> sparks.

### 500-Pos Intra-SR [Ca] Measurements In Rabbit Cardiomyocytes During Ca Transients And Waves

Timothy L. Domeier, Lothar A. Blatter

*Loyola University Chicago, Maywood, IL, USA.*

#### Board B348

We used the low-affinity Ca indicator Fluo-5N to monitor dynamic changes in sarcoplasmic reticulum [Ca] ([Ca]<sub>SR</sub>) in isolated rabbit atrial and ventricular myocytes. During field stimulation-induced Ca transients (1 Hz), Fluo-5N fluorescence decreased to 66% (atrial myocytes) and 64% (ventricular myocytes) of the caffeine-sensitive Fluo-5N fluorescence (F<sub>Caff</sub>). In atrial cells exhibiting spontaneous cytosolic Ca waves, Fluo-5N reported intra-SR Ca depletion waves with depletion amplitudes to 46% of F<sub>Caff</sub>. Increasing pacing frequency from 0.5 to 1 Hz resulted in an increase in diastolic [Ca]<sub>SR</sub> and Ca transient depletion amplitude in atrial and ventricular myocytes. In atrial myocytes the change in pacing frequency also resulted in the brief (~30 s) appearance of depletion alternans. To determine the [Ca]<sub>SR</sub>-dependence of Ca release during electrically evoked Ca transients, ventricular myocytes were stimulated with a single pulse at variable levels of [Ca]<sub>SR</sub>. [Ca]<sub>SR</sub> was manipulated by passive leak after variable periods of rest or by application of caffeine (10 mM). [Ca]<sub>SR</sub> depletion transients (Δ[Ca]<sub>SR</sub>) were detected at a minimum diastolic [Ca]<sub>SR</sub> of ~0.5 mM, and the magnitude of Δ[Ca]<sub>SR</sub> steadily increased with diastolic [Ca]<sub>SR</sub>. The relationship between Δ[Ca]<sub>SR</sub> and diastolic [Ca]<sub>SR</sub> was similar whether [Ca]<sub>SR</sub> was experimentally altered via rest decay or by caffeine application. Minimum [Ca]<sub>SR</sub> during electrical stimulation varied with diastolic [Ca]<sub>SR</sub>, showing that global SR Ca release did not terminate at a set [Ca]<sub>SR</sub>. Application of the β-adrenergic agonist Isoproterenol (10<sup>-6</sup> M) increased diastolic [Ca]<sub>SR</sub> during pacing and dramatically enhanced the rate of SR Ca uptake. However, at [Ca]<sub>SR</sub> < 1.5 mM, Isoproterenol did not appreciably alter the relationship between Δ[Ca]<sub>SR</sub> and diastolic [Ca]<sub>SR</sub>. These data suggest that for a given SR Ca content β-adrenergic stimulation does not alter fractional SR Ca release.

### 501-Pos SALVO- A New Analytical Platform For Decoding Intracellular Ca<sup>2+</sup> Fluxes And Evaluating Novel Anti-arrhythmic Compounds

Steven R. Barberini<sup>1</sup>, Philip M. Ashton<sup>1</sup>, William C. Claycomb<sup>2</sup>, F. Anthony Lai<sup>1</sup>, Christopher H. George<sup>1</sup>

<sup>1</sup> *Cardiff University, Cardiff, United Kingdom*

<sup>2</sup> *Louisiana State University Health Sciences Center, New Orleans, LA, USA*

**Board B349**

The complexities of  $\text{Ca}^{2+}$  signalling dysfunction in cardiac disease predicts diverse targets for therapeutic modulation. Pharmacological approaches to normalise cardiac function are rapidly moving towards strategies based on rational design and unbiased phenotypic analysis to identify novel and more effective compounds. However, a major obstacle in cardiac drug development stems from the routine use of 'industrial standard' cell types (e.g. CHO, HEK and NIH-3T3 cells) in high-throughput screening (HTS) strategies that bear little physiological relevance to the cardiac environment and do not recreate the synergistic nature of cardiac ion handling. Consequently, the systematic identification and evaluation of new and improved drugs that lie buried in vast chemical libraries is critically dependent on developing physiologically relevant, cardiomyocyte-based platforms. We have established a bioassay based on high-resolution confocal  $\text{Ca}^{2+}$  imaging of spontaneously beating, functionally coupled monolayers of HL-1 cardiomyocytes grown to high density on a gelatin-fibronectin matrix. Data from this cellular syncytium is analysed using SALVO, a multi-parametric algorithm package that quantifies diverse aspects of cellular  $\text{Ca}^{2+}$  cycling and  $\text{Ca}^{2+}$  transient profiles (including synchrony, amplitude, length, variability, oscillation) and decodes the spatio-temporal encryption of  $\text{Ca}^{2+}$  signals that underpin cardiac rhythmicity, synchrony and contractility at single and multi-cellular levels. Proof-of-principle experiments using a well characterised pro-arrhythmic stimulus (ouabain) have demonstrated the robust utility of this platform to evaluate the potential therapeutic efficacy and mechanisms of action of compounds including

1. AAP10, a hexapeptide that increases cellular synchrony via enhanced gap junctional communication,
2. 2-APB, a broad specificity ion-channel modulator and
3. mimetic peptides that modulate connexin hemi-channel permeability.

This system represents the first cardiomyocyte-based platform that is suitable for HTS applications and provides a powerful approach for evaluating novel anti-arrhythmic compounds.

**502-Pos Does enhanced SR Ca buffering induce systolic  $[\text{Ca}^{2+}]_i$  alternans?**

Yatong Li, Stephen O'Neill, David Eisner

*University of Manchester, Manchester, United Kingdom.*

**Board B350**

Overexpression of the SR Ca buffer calsequestrin (CSQ) results in mechanical alternans (Schmidt et al *J. mol. cell. cardiol.* 32, 1735). We have previously shown that alternans (produced by decreasing SR Ca release) is associated with propagation of Ca waves (Díaz *et al. Circ Res* 94, 650). Citrate binds Ca with low affinity and can enter the SR to act as a Ca buffer. The aim of this work was to investigate if this addition of buffer to the SR could produce systolic  $[\text{Ca}^{2+}]_i$  alternans and by what mechanism. Rat myocytes were stimulated by a 100ms pulse to 0mV from a holding potential of -40 mV using the whole cell configuration at room temperature. 60mM citrate and 50 $\mu\text{M}$  Fluo-3 were included in the pipette solution. Early after going

whole cell, depolarization activated spatially uniform systolic Ca transients. As more citrate dialysed into the cell, beat to beat alternans gradually developed in Ca transient and currents. The larger Ca transients were associated with smaller Ca currents. On average the L-type Ca current associated with a small Ca transient allowed the entry of  $4.0 \pm 0.14$  compared to  $2.96 \pm 0.41$   $\mu\text{mol/l}$  Ca for that with the larger transient. The efflux on NCX was  $3.51 \pm 0.13$  for the small transient and  $16.9 \pm 0.8$   $\mu\text{mol/l}$  for the large (n=6). Therefore the cell (and presumably the SR) Ca content will vary by about 14  $\mu\text{mol/l}$  during alternans. The small Ca transients had only a single, rapid rising phase. However large ones showed a second slow phase of rise due to propagation of Ca waves. Like alternans produced by decreasing SR Ca release, that due to citrate is associated with beat to beat changes of cell Ca content and depends on Ca wave propagation.

**503-Pos Action Potential Prolongation and T-tubule Disorganization Promote Slowing of  $\text{Ca}^{2+}$  Release in Failing Murine Cardiomyocytes**

William E. Louch, Halvor K. Mork, Karina Hougen, Taevje A. Stromme, Ivar Sjaastad, Ole M. Sejersted

*University of Oslo, Oslo, Norway*

**Board B351**

Cardiomyocytes from failing hearts exhibit slowing of the rising phase of the  $\text{Ca}^{2+}$  transient. Decreased sarcoplasmic reticulum (SR)  $\text{Ca}^{2+}$  content likely contributes to this deficit. However, slowing of SR  $\text{Ca}^{2+}$  release may also result from decreased release synchrony, due to alterations in action potential (AP) or T-tubule configuration. We examined whether these mechanisms coexist in a murine model of congestive heart failure (CHF). Myocardial infarction was induced by left coronary artery ligation and, at 10 weeks following surgery, mice exhibited clear symptoms of CHF. SHAM-operated mice served as controls. Cardiomyocytes isolated from viable regions of the septum exhibited markedly slower  $\text{Ca}^{2+}$  transients (fluo-4 AM, 1 Hz) in CHF than SHAM (time-to-peak =  $44 \pm 3$  ms vs  $26 \pm 1$  ms,  $P < 0.05$ ). Confocal line-scan images showed that SR  $\text{Ca}^{2+}$  release was also less synchronous in CHF. AP duration was significantly prolonged in CHF cells at 50, 70, and 90% repolarization ( $P < 0.05$ ) due to reduced transient outward and steady-state  $\text{K}^+$  currents. However, APs did not exhibit a notch during early repolarization which is critical for synchronizing  $\text{Ca}^{2+}$  release in larger mammals. Indeed,  $\text{Ca}^{2+}$  release synchrony was similar during voltage-clamp stimulation with the SHAM or CHF AP waveform. The CHF AP nevertheless prolonged the peak of the  $\text{Ca}^{2+}$  transient, increasing time-to-peak measurements by approximately 4 ms in both cell types. The T-tubule network (di-8-ANEPPS staining) was disorganized in CHF myocytes with irregular gaps between adjacent tubules. Regions of delayed  $\text{Ca}^{2+}$  release occurred at these gaps, increasing dyssynchrony of  $\text{Ca}^{2+}$  release. Thus, prolongation of the AP and T-tubule disorganization both contribute to the longer rise time of  $\text{Ca}^{2+}$  transients in CHF myocytes. However, AP prolongation in CHF mice does not decrease SR  $\text{Ca}^{2+}$  release synchrony as has been reported in larger mammals.



## 504-Pos $\text{Ca}^{2+}$ sparks alterations in type 2 diabetic mice. Is TNF- $\alpha$ involved?

Laetitia Pereira<sup>1</sup>, Gema Ruiz<sup>2</sup>, Sylvain Richard<sup>1</sup>, Carmen Delgado<sup>2</sup>, Ana M. Gomez<sup>1</sup>

<sup>1</sup>INSERM, U637, Montpellier, France

<sup>2</sup>Universidad Complutense de Madrid, Madrid, Spain.

### Board B352

We have previously shown that  $[\text{Ca}^{2+}]_i$  transients are reduced in cardiac myocytes from type 2 diabetic db/db mice. The  $[\text{Ca}^{2+}]$  transient is composed of the spatial and temporal summation of local events of  $\text{Ca}^{2+}$  release by functional clusters of RyRs, termed  $\text{Ca}^{2+}$  sparks. Using confocal microscopy, we analyzed  $\text{Ca}^{2+}$  sparks in 0.1% saponin permeabilized myocytes isolated from male mice. The  $\text{Ca}^{2+}$  spark frequency in diabetic (db/db) cells was significantly smaller than in control (+/+) cells (No. sparks/sec\*100  $\mu\text{m}$ :  $2.5 \pm 0.3$ ,  $n=27$  db/db vs  $5.1 \pm 0.7$ ,  $n=15$  +/+,  $p < 0.05$ ) while their amplitude was higher in db/db than in +/+ cells (peak  $F/F_0$ :  $2.2 \pm 0.02$  in +/+,  $n=1116$  v.s.  $2.4 \pm 0.03$  in db/db,  $n=617$ ;  $p < 0.001$ ).  $\text{Ca}^{2+}$  sparks time to peak (in ms:  $14.5 \pm 0.3$  in +/+ v.s.  $13.0 \pm 0.4$  in db/db,  $p < 0.01$ ) and duration at half maximum ( $17.0 \pm 0.2$  in +/+ v.s.  $14.6 \pm 0.3$  in db/db,  $p < 0.001$ ) was accelerated in db/db myocytes.  $\text{Ca}^{2+}$  spark spatial spread was limited in db/db myocytes (in  $\mu\text{m}$ :  $1.3 \pm 0.0$  in +/+ v.s.  $1.2 \pm 0.0$  in db/db,  $p < 0.001$ ). It has been suggested that the inflammatory cytokine TNF- $\alpha$  is increased in diabetes. Using western-blot we investigated the cardiac expression level of TNF- $\alpha$  receptors type 1 (TNF-R1) and 2 (TNF-R2) and the TNF- $\alpha$  converting enzyme (TACE). While TNF-R1 was similar in +/+ and db/db hearts, TNF-R2 and TACE expressions were increased in db/db hearts. We analyzed the effects of TNF- $\alpha$  on  $\text{Ca}^{2+}$  handling. In control myocytes 30 min incubation with 10 ng/ml TNF- $\alpha$  decreased  $[\text{Ca}^{2+}]_i$  transients ( $F/F_0$ :  $2.2 \pm 0.1$  in 16 control cells vs.  $1.8 \pm 0.1$  in 8 TNF- $\alpha$  cells). In conclusion, we found that  $\text{Ca}^{2+}$  sparks frequency and characteristics are altered in db/db cardiac myocytes, and that the TNF- $\alpha$  signalling is enhanced in db/db hearts. Further analyses are required to determine whether a link exists between these two findings.

## 505-Pos Differential Effects Of ATP On $\text{Ca}^{2+}$ Regulation By The Golgi Apparatus And SR In Rat Ventricular Myocytes

Derek S. Steele, Zhaokang Yang

University of Leeds, Leeds, United Kingdom

### Board B353

In previous studies we have described prolonged  $\text{Ca}^{2+}$  release (PCR) events, which arise close to the nucleus in ventricular cells and influence nucleoplasmic  $[\text{Ca}^{2+}]$ . PCR occurs spontaneously and exhibits a sustained plateau phase lasting  $1.78 \pm 0.19$  seconds ( $n=6$ , mean  $\pm$  S.E.M.) and a width at half maximum amplitude of  $5.0 \pm 0.2$   $\mu\text{m}$  ( $n=6$ ). Structural evidence suggests that PCR originates from the Golgi apparatus (GA). This conclusion is supported by experiments showing that disruption of the GA with ilimaquinone (25  $\mu\text{M}$ )

abolishes PCR, while SR  $\text{Ca}^{2+}$  release is unaffected. In the present study, the effects of cytosolic ATP on  $\text{Ca}^{2+}$  release by the GA and the SR were compared in rat ventricular myocytes. Cells were permeabilized with saponin during exposure to a mock intracellular solution containing 150 nM free  $[\text{Ca}^{2+}]$  and 20  $\mu\text{M}$  fluo-3 (20 °C). Under these  $\text{Ca}^{2+}$  loading conditions, SR derived  $\text{Ca}^{2+}$  sparks were apparent in all cells, although only 1/13 cells exhibited PCR. In all cells, decreasing the [ATP] from 5 to 0.05 mM caused a sustained reduction in spark frequency (by  $71 \pm 4\%$ ,  $n=8$ ). However, in cells not exhibiting PCR, the decrease in [ATP] induced repeated PCR events in 7 of 11 cells. Furthermore, in intact myocytes superfused with Tyrode's solution, metabolic inhibition with cyanide (0.5 mM) induced repeated PCR, in 5 of 8 cells. These data suggest that in adult myocytes

- (i) the GA operates acts as a  $\text{Ca}^{2+}$  store that is functionally distinct from the SR
- (ii) GA and SR  $\text{Ca}^{2+}$  release are differentially regulated by cytosolic ATP.

Activation of GA induced  $\text{Ca}^{2+}$  release by ATP depletion suggests a role in modulation of nuclear  $[\text{Ca}^{2+}]$  during metabolic impairment.

## 506-Pos Measurement of SR Ca Accumulation in Sarolemma Permeablized Rabbit Myocytes Using the Low Affinity Ca-Dependent Dye Fura2

Stephen Shonts<sup>1</sup>, Thomas R. Shannon<sup>1</sup>, Donald M. Bers<sup>2</sup>

<sup>1</sup>Rush University Medical Center, Chicago, IL, USA

<sup>2</sup>Loyola University Medical Center, Maywood, IL, USA

### Board B354

In cardiomyocytes proper function of Ca transport and sequestration are essential mechanisms of both Ca homeostasis and contractility. Central to these mechanisms is the sarcoplasmic reticulum (SR) and its ability to sequester Ca via the Ca pumps. This sequestration depends upon both the speed of uptake and the gradient for Ca across the membrane which can be established. The latter has been characterized only in SR vesicles (Shannon et al, *Biophysical J.* 73:1524–1531). Here we measure the free intrasarcoplasmic reticulum  $[\text{Ca}]$  ( $[\text{Ca}]_{\text{SR}}$ ) in isolated rabbit cardiac myocytes. The SR of the ventricular myocytes was loaded with the low-affinity Ca indicator fura2. The sarcolemma (SL) of the myocytes was permeabilized by 0.0025% saponin in a Ca-free internal solution to prevent SR Ca uptake. This was done in order to expose the cytosol to extracellular solutions and to allow cytosolic fura2 to diffuse out of the cell. SR Ca release channels were blocked by the presence of 1 mM tetracaine. FCCP and oligomycin were used to inhibit uptake of Ca into mitochondria. SR Ca uptake was then initiated by addition of a solution containing 25 nM Ca and 5 mM ATP. Stepwise increases in  $[\text{Ca}]_i$  up to 300 nM in the presence of ATP caused progressive increases in steady-state fluorescence ration (excitation = 340/380 nm) indicating a rise in  $[\text{Ca}]_{\text{SR}}$ . The process continued until  $R_{\text{max}}$   $0.63 \pm 0.02$  SEM, ( $n=3$ ) was reached.  $R_{\text{min}}$   $0.34 \pm 0.03$  was established by exposure to 10mM caffeine. Future experiments aim to establish a fluorescence calibration to

determine the in situ  $K_d$  of furaptra and a subsequent measure of intra-SR [Ca], thus allowing the establishment of the steady-state SR Ca pump efficiency in cardiac myocytes.

### Voltage-gated K Channels - I

## 507-Pos C-type Inactivation From The Perspective Of Permeant Ions

Sudha Chakrapani<sup>1</sup>, Julio F. Cordero-Morales<sup>1,2</sup>, Luis G. Cuello<sup>1</sup>, Eduardo Perozo<sup>1</sup>

<sup>1</sup> University of Chicago, Chicago, IL, USA

<sup>2</sup> University of Virginia, Charlottesville, VA, USA.

### Board B355

KcsA is widely accepted to enclose a prototype of  $K^+$ -selective pathway and has provided a structural-framework to understand selectivity, ion-permeation, gating and pore-blocking. Recently identified C-type inactivation in KcsA further strengthens its role as an archetypical pore of Kv channels. In an attempt to tease-out the fine details of the inactivation mechanism in KcsA, we have carried out a systematic analysis of macroscopic and single-channel currents under varying conditions of pH, voltage, permeant-ions and blockers. We find that KcsA inactivation is modulated by voltage and recovery occurs predominantly via closure of the lower activation-gate. Inactivation in KcsA is not entirely a property of the open-conducting channel but also occurs from partially "activated"-closed-states with rates progressively increasing from the farthest closed-state to the open-state suggesting a strong coupling between activation and inactivation. Recovery experiments demonstrate that when preceded by high-throughput ion-permeation, inactivation occurs faster and to a much deeper extent (compared to without ion-conduction in the absence of a driving force). Further, inactivation rates also vary as a function of the amount of current passing through the channel; these results reveal a greater tendency of the filter to collapse while the ions transition from one binding-site to the next. This collapse, as suggested in previous studies, likely involves a constriction at the external binding-site and is favored under low external  $K^+$  where inactivation is significantly faster. Consistent with this idea, ions with long residence-time in the filter ( $Rb^+$ ,  $Cs^+$ ,  $Ba^{2+}$ ) dramatically slow-down inactivation, a property closely reflecting the "foot-in-the-door" effect observed in Kv channels. As also implicated by studies in eukaryotic channels, C-type inactivation in KcsA appears to involve an intimate interplay between the selectivity-filter region and permeant-ions. We analyze these findings in the light of new high-resolution structural information on the inactivated-states.

## 508-Pos A Multi-point Hydrogen Bond Network Driving Kcsa C-type Inactivation

Julio Francisco Cordero-Morales<sup>1,2</sup>, Sudha Chakrapani<sup>2</sup>, Vishwanath Jogini<sup>2</sup>, Eduardo Perozo<sup>2</sup>

<sup>1</sup> University of Virginia, Charlottesville, VA, USA

<sup>2</sup> University of Chicago, Chicago, IL, USA

### Board B356

The prokaryotic proton-gated potassium channel KcsA undergoes a time dependent slow inactivation process, which is modulated by transmembrane voltage but not by pH. Previous results have suggested that the number and strength of hydrogen bonds between residues in the pore helix and external vestibule determine the rate and extent of the C-type inactivation. The interaction between Glu71 and Asp80 is one of the key driving forces that promote filter instability through a compression of the selectivity filter parallel to the permeation pathway, which energetically biases it towards the inactivated conformation. High resolution KcsA structures suggest that the selectivity filter is also stabilized by an interaction between Trp67 and Asp80, a partnership conserved in most potassium channels. Using patch clamp experiments, EPR spectroscopy and X-ray crystallography, we have studied the effect of amino acid substitutions at position 67, in an attempt to establish the role of this residue in the inactivation gating at the selectivity filter of KcsA. Substitution of Trp67 to phenylalanine decreases the rate and extent of inactivation as determined by macroscopic and single channel currents. Thus, as in the Glu71-Asp80 interaction, disrupting the interaction between residues Trp67 and Asp80 unmasks the presence of another critical hydrogen bond at the selectivity filter of KcsA. Indeed, sequence alignment of several prokaryotic potassium channels suggests tyrosine as the natural amino acid substitution at this position. Furthermore, substitution to tyrosine (W67Y) recovered the inactivation phenotype presumably by reestablishing the 67 and Asp80 interaction through a hydrogen bond. Taken together, the present results suggest that in addition to the Glu71 and Asp80 carboxyl-carboxylate interaction, the hydrogen bond between Trp67 and Asp80 at the KcsA selectivity filter and its adjacent pore helix constitutes another key interaction that determines the rate and extent of C-type inactivation.

## 509-Pos Gating-related Conformational Changes in the Outer Vestibule of KcsA: A Functional and Spectroscopic Analysis

H. Raghuraman, Julio F. Cordero-Morales, Eduardo Perozo  
*Institute for Molecular Pediatric Sciences, The University of Chicago, Chicago, IL, USA.*

### Board B357

The potassium channel KcsA is gated by proton and modulated by the transmembrane voltage. It is well established that there is a large conformational change in the lower gate of KcsA upon change in pH. In addition, it has been shown that the selectivity filter also play a crucial role as a second gate in ion conduction. The high sequence similarity between KcsA and eukaryotic potassium channels at the p-loop region makes it a suitable model system for studying the conformation changes associated with the gating. In this study, we have monitored the conformational changes in the outer vestibule of KcsA during gating using electrophysiological and spectroscopic (EPR and fluorescence) measurements. We generated several cysteine mutants corresponding to the outer vestibule of full-length KcsA using wild type and E71A mutant backgrounds (representing the inactivated and non-inactivated states of KcsA), to understand the gating-related conformational changes. Our EPR mobility